

CEBAF PROPOSAL COVER SHEET

This Proposal must be mailed to:

CEBAF
Scientific Director's Office
12000 Jefferson Avenue
Newport News, VA 23606

and received on or before OCTOBER 31, 1989

A. TITLE: Electroproduction of the P_{33} (1232) Resonance

B. CONTACT PERSON: Volker Burkert

ADDRESS, PHONE AND BITNET:

CEBAF 804/249-7540
BURKERT@cebafvax

C. THIS PROPOSAL IS BASED ON A PREVIOUSLY SUBMITTED LETTER OF INTENT

YES
 NO

IF YES, TITLE OF PREVIOUSLY SUBMITTED LETTER OF INTENT

A Measurement of the Electromagnetic Transition Multipoles for Single Pion Electroproduction in the Mass Region of the (1232) Resonance for $Q^2 \leq 4(\text{GeV}/c)^2$.

D. ATTACH A SEPARATE PAGE LISTING ALL COLLABORATION MEMBERS AND THEIR INSTITUTIONS

=====
(CEBAF USE ONLY)

Proposal Received 10-31-89

Log Number Assigned PR-89-037

By KES
contact: Burkert

**Study of Electromagnetic Excitation of Baryon Resonances
with the CEBAF Large Acceptance Spectrometer**

The N* Collaboration

V. Burkert, D. Joyce, B. Mecking, M.D. Mestayer, B. Niczyporuk,
E.S. Smith, A. Yegneswaran
CEBAF, Newport News, Virginia

R. Minehart, D. Day, J. McCarthy, O. Rondon-Aramayo, R. Sealock,
S. Thornton, H.J. Weber
University of Virginia, Charlottesville, Virginia

P. Stoler, G. Adams, L. Ghedira, N. Mukhopadyay
Rensselaer Polytechnic Institute, Troy, New York

R. Arndt, D. Jenkins, D. Roper
Virginia Polytechnic Institute and State University, Blacksburg, Virginia

D. Isenhower, M. Sadler
Abilene Christian University, Abilene, Texas

D. Keane, M. Manley
Kent State University, Kent, Ohio

S. Dytman, T. Donoghue
University of Pittsburg, Pittsburg, Pennsylvania

C. Carlson, H. Funsten
College of William and Mary, Williamsburg, Virginia

D. Doughty
Christopher Newport College, Newport News, Virginia

L. Dennis, K. Kemper
Florida State University, Tallahassee, Florida

K. Giovanetti
James Madison University, Harrisonburg, Virginia

J. Lieb
George Mason University, Fairfax, Virginia

W. Kim
University of New Hampshire, Durham, New Hampshire

C. Stronach
Virginia State University, Petersburg, Virginia

M. Gai
Yale University, New Haven, Connecticut

Proposal 1

Electroproduction of the $P_{33}(1232)$ Resonance.

The N^{*} Group

- in the CLAS Collaboration -

G. Adams, R. Arndt, V. Burkert, C. Carlson, L. Dennis, D. Day, D. Doughty, T. Donoghue, S. Dytman, D. Isenhower, H. Funsten, M. Gai, L. Ghedira, K. Giovanetti, D. Jenkins, D. Joyce, D. Keane, K. Kemper, W. Kim, J. Lieb, M. Manley, J. McCarthy, B. Mecking, M.D. Mestayer, R. Minehart, N. Mukhopadhyay, B. Niczyporuk, O. Rondon-Aramayo, D. Roper, M. Sadler, R. Sealock, E.S. Smith, P. Stoler, C. Stronach, S. Thornton, H.J. Weber, and A. Yegneswaran.

Spokespersons: V. Burkert, R. Minehart.

Abstract

We propose to carry out measurements with the CLAS detector aimed at obtaining precise information on the electric, magnetic, and scalar/longitudinal multipoles E_{1+} , M_{1+} , S_{1+} transition in the mass region of the $\Delta(1232)$. These multipoles characterize the resonant transition into the excited $\Delta(1232)$ state. We will also get information on the nonresonant multipoles S_{0+} , E_{0+} , M_{1-} , in the mass range of the $\Delta(1232)$ resonance. The resonant multipoles are a sensitive probe of the structure of the excited $\Delta(1232)$ state. Precise knowledge of these multipoles allow discrimination between models of the nucleon structure. We propose to use two beam energies of 2 GeV and 4 GeV to cover the Q^2 range from 0.2 to 4.0 GeV². Complete azimuthal and polar angle distribution of the reaction $p(e, e'p)\pi^0$, $p(e, e'\pi^+)n$, and $D(e, e'\pi^-)pp_s$ will be measured. In a second and third stage we want to carry out measurements using a polarized electron beam, and a polarized target, respectively.

I. Motivation.

The $P_{33}(1232)$ or $\Delta(1232)$ resonance is of special interest to nuclear physics as well as to particle physics. It is the most prominent resonance in electromagnetic interactions at low and modestly high Q^2 and plays an important role in electron scattering from nuclei at intermediate energies. Because of its prominent character is the $\Delta(1232)$ most suitable for studying interaction of resonances and possible modification of resonance parameters in the nuclear medium. It is quite clear that such a study requires that these parameters are precisely enough known for free nucleons.

In recent years there has been a dramatic increase in the number of theoretical papers dealing with photo- and electroproduction of the $\Delta(1232)$ and other baryon resonances¹⁻¹⁵, indicating a renewed interest in the study of baryon structure using electromagnetic probes. The central issue of the electromagnetic excitation of the $\Delta(1232)$ is the $\gamma N \Delta$ vertex which is a sensitive probe of the internal baryon structure. Earlier experiments revealed the dominant magnetic character of the $\gamma N \rightarrow \Delta(1232)$ transition. The $\gamma N \Delta$ coupling is described by a magnetic dipole transition M_{1+} . In quark models, which are based on $SU(6)_w$ symmetry, this is explained by a spin flip of one of the constituent quarks in the $L_{3Q}=0$ state of the 3-Quark wave function³⁹. Within these models are the scalar (longitudinal) and electric quadrupole transition into the $\Delta(1232)$ predicted to be 0 for all momentum transfers. In more elaborate models, which include color magnetic effects arising from the QCD motivated one-gluon exchange between quarks¹⁶, small nonmagnetic contributions in terms of electric (E_{1+}) and scalar (S_{1+}) quadrupole transitions arise². These correspond to transitions into the $SU(6)$ forbidden, nonspherical $L_{3Q}=2$ state. In the static limit this is interpreted as the result of a quadrupole deformation of the $\Delta(1232)$. By measuring the Q^2 dependence of the electromagnetic multipoles we obtain information on the relative importance of these components as a function of the distance probed. Measurements of the scalar and electric quadrupole transition multipoles provide sensitive means of discriminating between various microscopic models of the nucleon.

I.1 The Ratio E_{1+}/M_{1+} - Electric Quadrupole Transition.

Here we use the definition $R_{EM} = E_{1+}/M_{1+}$. The small value of $R_{EM} \simeq -0.015$ found in analyses of pion photoproduction data gives some indication that a small quadrupole deformation of the $\Delta(1232)$ may indeed exist. On the other hand this value is still uncertain at roughly the same magnitude (see Ref. [40] for a recent review). Theoretical calculations of the Q^2 dependence of the transition amplitudes of the $\Delta(1232)$ have been done within the framework of various dynamic quark models^{7,10,17,18}. All of these calculations predict that E_{1+}/M_{1+}

either is identically 0, or remain small up to large values of Q^2 . Figure 1 displays the result of some recent calculations. Note that $E_{1+}=0$ corresponds to $A_{\frac{1}{2}} = 1/(\sqrt{3})A_{\frac{3}{2}}$ for the photocoupling helicity amplitudes (defined in the Appendix) and $A(\Delta) = -\frac{1}{2}$ for the helicity asymmetry.

$$A = \left(A_{\frac{1}{2}}^2 - A_{\frac{3}{2}}^2 \right) / \left(A_{\frac{1}{2}}^2 + A_{\frac{3}{2}}^2 \right).$$

In sharp contrast to the explicit quark model calculations the perturbative QCD (pQCD) predicts that

$$R_{EM} \rightarrow 1 \text{ at high } Q^2$$

(corresponding to $A_{\frac{3}{2}}/A_{\frac{1}{2}} \rightarrow 0$), and therefore

$$A(\Delta(1232)) \rightarrow +1.$$

The $\Delta(1232)$ is, in fact, the only prominent resonance where dynamical quark model calculations and pQCD give qualitatively different predictions for the $\gamma p \Delta^*(1232)$ helicity asymmetry $A(\Delta)$. For other prominent resonances the helicity asymmetry is predicted to approach unity at high Q^2 both in dynamical quark model calculations and in pQCD.

Another intriguing aspect of the $N \rightarrow \Delta$ transition for high Q^2 is its sensitivity to the nucleon distribution amplitude. Distribution functions have been determined using QCD sum rules. C. Carlson¹⁹ has shown that for the asymptotic value of isospin $\frac{3}{2}$ and $\frac{1}{2}$ resonances

$$A_{\frac{1}{2}}(\Delta) \ll A_{\frac{1}{2}}(N^*) \text{ at large } Q^2.$$

should hold, if the distribution amplitudes of Chernyak-Zhitnisky²⁰ or King-Sachrajda²¹ are correct. The same is not the case for the distribution function of Gari-Stefanis²². It is therefore important to compare the resonance transitions to isospin $\frac{1}{2}$ and $\frac{3}{2}$ resonances at large Q^2 .

At what values of Q^2 can one expect to observe the onset of asymptotic behaviour? Arguments have been made¹⁹ that asymptotic behaviour may already be seen for Q^2 values as low as 4 - 5 GeV². However, in other models like the Generalized Vector Meson Dominance Model of Koerner¹³, which also incorporates the correct asymptotic Q^2 dependence, the onset of asymptotic behaviour for the $\gamma_p \Delta(1232)$ transition is predicted to occur at much larger values of Q^2 . Isgur and Llewellyn-Smith³⁶ also discussed this issue with respect to the Q^2 dependence of the nucleon form factor and reached similar conclusions. The resolution of this controversy will be greatly facilitated by the experiments we are proposing. Even if the proposed experiment cannot reach Q^2 values in excess

of 3 (or 4 GeV²), the trend of the data at such Q² values should help settle the controversy about the applicability of pQCD methods at modestly high Q². At the least, R_{EM} should be positive, and should have assumed a much larger value than at low Q² if pQCD methods are applicable in this Q² regime.

In the limit $Q^2 \rightarrow 0$, R_{EM} was found to be sensitive to the size of the quark confinement region. Using the Cloudy Bag Model (CBM) Bermuth et al.⁵ found that R_{EM} is very sensitive to the bag radius. R_{EM} is predicted to vary by a factor of 2 for bag radii from 0.7 to 1 fm. For smaller bag radii the pion cloud contribution becomes more important and is responsible for a large portion of R_{EM} . On the other hand the dominant $\langle 1_+ \rangle$ multipole is predicted to be almost independent of the bag radius.

Recently S. Kumano⁶ has shown that pionic contributions to the $\gamma_\nu N \Delta$ electric quadrupole formfactors are sizeable, and might be larger than contributions from the “quark core”. These contributions also lead to a shift in the phases of the respective multipoles, such that

$$R_{EM} = (+0.014 - 0.057i) \text{ at } Q^2 = 0 .$$

For comparison, the non-relativistic quark model gives³

$$R_{EM} \simeq -0.004 \text{ at } Q^2 = 0 .$$

and the relativized quark model yields¹⁰

$$R_{EM} \simeq -0.013 \text{ at } Q^2 = 0 .$$

The pionic contributions are predicted to be much larger for the $\gamma_\nu p \rightarrow \pi^+ n$ channel than for the $\gamma_\nu p \rightarrow p \pi^0$ channel.

It will be very interesting to see how the value of R_{EM} changes when Q² changes from low values to intermediate and high values. If, as in the model of Kumano, E_{1+} is largely determined by the pion cloud of the nucleon, then it should exhibit a Q² dependence that reflects the larger size of the pion cloud compared to the quark “core”. Predictions of R_{EM} are shown in Figure 1. Precise measurements over a wide Q² range should prove extremely powerful in discriminating between the various microscopic models.

1.2 The Ratio $S_{1+}/M_{1+} - \gamma_\nu p \Delta$ Coulomb Transition.

In SU(6)_W symmetric quark models R_{EM} (we define $R_{SM} = S_{1+}/M_{1+}$) should be zero. The inclusion of QCD motivated one-gluon exchange between valence quarks¹⁶ leads to a finite longitudinal (scalar) coupling in the $\gamma_\nu p \rightarrow \Delta(1232)$

transition³. Theoretical predictions are shown in Figure 1. In the QCD extended version of the non-relativistic quark model, R_{SM} is predicted to vary from $\simeq -0.01$ to -0.06 in the Q^2 range from 0. to 3.0 GeV^2 . The relativized quark model of Warns et al.¹⁰ yields values for R_{SM} ranging from $+0.005$ to $+0.018$ in this Q^2 range. Perturbative QCD, predicts $R_{SM} \rightarrow 0$ for asymptotically large Q^2 . Precise measurements of R_{EM} up to the $Q^2 \simeq 4 \text{ GeV}^2$ should allow discrimination between these models.

1.3 Previous Measurements

The longitudinal and electric quadrupole coupling in the $\gamma_p \Delta(1232)$ transition has been studied experimentally in inclusive electron proton scattering²³, and in exclusive π^0 electroproduction²⁴. The experiments were carried out in the early 1970's at electron synchrotron laboratories like CEA, DESY, NINA and Bonn, and were primarily geared towards establishing the dominant contributions and the approximate magnitudes of the small multipoles. The experiments are discussed in the review article by Foster & Hughes⁴⁰, and most recently by Papanicolas⁴¹. At the time when the early measurements were performed, only predictions of quark models which were based on exact $SU(6)_w$ symmetry existed, yielding $S_{1+} = E_{1+} = 0$. Consequently, there was no reason to improve the precision of the experiments. The inclusive data (Figure 2) cover the Q^2 range from 0.3 to 0.6 GeV^2 , and are compatible with $\sigma_L/\sigma_T=0$ near the resonance mass. Obviously, even data with improved statistical accuracy would not allow one to distinguish between resonant and nonresonant contributions.

Exclusive single pion production is more sensitive to smaller amplitudes via interference effects, and also allows a much better discrimination of nonresonant contributions. The $p(e, e'p)\pi^0$ data give results which are consistent with a small negative value of R_{SM} (Figure 3). For R_{EM} the various experiments give absolute values < 0.05 (Figure 4). However, they are inconsistent with each other regarding the magnitude and sign of R_{EM} . The published data are limited to $Q^2 < 1 \text{ GeV}^2$ and generally do not discriminate between resonant and nonresonant contributions. In the analyses M_{1+} dominance was generally assumed, and only terms in the cross section containing the M_{1+} multipole were retained. In addition, only s- and p- wave contributions were included in the partial wave expansion of the cross section. Under these assumptions one can determine the magnetic dipole term $|M_{1+}|$, and the interference terms $\text{Re}(S_{1+}M_{1+}^*)$, $\text{Re}(S_{0+}M_{1+}^*)$, and $R_{EM}(E_{0+}M_{1+}^*)$. From the first and third terms one can determine R_{SM} and R_{EM} , if the multipoles contain only resonant contributions to the $\Delta(1232)$ excitation (Watson's theorem). This, however, is not necessarily the case if one looks at only one isospin channel as in the case of π^0 production. In fact, calculations using dispersion relation methods predict sizeable nonresonant contributions to S_{1+} in the $I=1/2$ channel²⁵ which have to be taken into account when analyzing the data. Such contributions would lead to a change in the phase relation

between the S_{1+} and M_{1+} multipoles. Isospin 1/2 and 3/2 contributions can be disentangled if pion production in different isospin channels is investigated.

II. Proposed Measurements.

The measurements we propose to perform are geared towards improving the experimental situation to a point where the resonant multipoles can be extracted with high accuracy. The experimental program includes differential cross section measurements in different isospin channels like

$$p(e, e'p)\pi^0 \quad (1)$$

$$p(e, e'\pi^+)n \quad (2)$$

which can be carried out simultaneously, and

$$D(e, e'\pi^-)pp_s, D(e, e'\pi^+)nn_s \quad (3)$$

where the subscript s identifies the spectator nucleon. From this set of measurements we obtain the complete isospin information on single pion production from nucleons in the $\Delta(1232)$ region. We assume that it will be possible to correct for nuclear effects in reaction (3). Information from the latter reaction is not required for identifying the resonant state (note that only one isospin amplitude can contribute to the $\Delta(1232)$ excitation). However, the additional information will be important in a complete analysis intended to separate the resonant and nonresonant contributions. For the latter contributions $I=1/2$ and $3/2$ are possible in the final state, so that 3 isospin amplitudes can contribute, which can be separated by measuring the channels mentioned above.

III. Expected Performance of CLAS.

III.1 Missing Mass Method

In the proposed measurement the final state is identified by the 4-momentum vector (mass and 3-momentum) of the detected charged particles. The exclusive reaction is then determined by employing the missing mass method. The mass of the unmeasured reaction products is given by

$$M_x^2 = (e + p - e' - p')^2$$

or

$$M_x^2 = (e + p - e' - \pi^+)^2$$

where e, e', p, p', π^+ are the 4-momenta of the respective particles.

We have studied the missing mass resolution of the CLAS detector for the various final states, using the CELEG event generator and the detector performance as implemented in the CLAS FASTMC Monte Carlo package. CELEG²⁷ generates events according to a parameterization of the inclusive $ep \rightarrow eX$ cross section, which incorporates all known non-strange baryon resonances. The parameters have been fitted to total photoproduction cross section data. The Q^2 dependence has been implemented using a parameterization by Brasse²⁶. The FASTMC package contains parametrizations of resolutions and acceptances of the CLAS detector²⁸.

As examples, Figure 5 and Figure 6 show the generated invariant mass spectra for a 4 GeV incident electron beam $Q^2 = 1 \text{ GeV}^2$. Using FASTMC the missing mass spectra for the reactions

$$e + p \rightarrow e' + p' + X$$

and

$$e + p \rightarrow e' + \pi' + X$$

were obtained, folded with resolution and acceptance of the CLAS detector. Figure 7 displays the results. In either case the single pion production channel is clearly separated from the two pion production threshold. Figure 8-10 show the CLAS acceptance for $\Delta(1232)$ production, and for measurement of the $p\pi^0$ and $n\pi^+$ decay channels.

III.2 Expected Accuracy of the Cross Section Measurements.

For estimating count rates and running time we have assumed a luminosity of $L = 10^{34} \text{ cm}^{-2} \text{ sec}^{-1}$. We have also assumed that the CLAS magnet will be operated at full field. To study the rates and efficiencies for measurement of the $p\pi^0$ and $n\pi^+$ channels the CELEG and FASTMC packages were used and acceptance functions were obtained for $0.5 < Q^2 < 3 \text{ GeV}^2$ using a 4 GeV incident electron beam.

III.2.1 The $p(e, e')\pi^0$ Reaction.

We expect to improve the statistical significance of the $\gamma_p \rightarrow p\pi^0$ data at the average by at least an order of magnitude. Even for the best measured kinematics will the improvement be a factor of 3 to 5. For the first time a nearly complete coverage in W , Q^2 , θ and Φ will be achieved. Figure 11 illustrates the expected improvement in statistical accuracy, and in angular coverage. It should be noted that for this comparison we have chosen the best previously measured data at $Q^2=1 \text{ GeV}^2$.

III.2.2 The $p(e, e'\pi^+)n$ Reaction.

For the charged pion channels the improvement over previous measurements will be even more dramatic. This channel has been difficult to study in the past, since the π^+ is emitted over 4π , yielding small rates when conventional magnetic spectrometers are used. With the CLAS detector we can measure the full angular distribution of the $\gamma_p \rightarrow \pi^+ n$ channel both in azimuth and in polar angle. Previously, only cross section measurements near forward and backward angles for a few selected Q^2 values have been possible³⁵. Figure 12 displays data from previous experiments and the decisively improved quality of the expected data from the proposed measurement are shown. For the first time it will be possible to measure complete angular distributions in this channel, which will provide the data for a detailed partial wave decomposition.

III.2.3 The ${}^2\text{H}(e, e'\pi^-)pp_s$ and ${}^2\text{H}(e, e'\pi^+)nn_s$ Reactions.

Measurement of the $n(e, e'\pi^-)p$ channel provides additional information in a different isospin channel. In the $\Delta(1232)$ region scattering off neutron targets is not needed to identify the isospin $I=3/2$ resonant state, but it is relevant in discriminating resonant and nonresonant amplitudes. There exist only two relatively low statistics measurements of the π^-/π^+ ratio in ${}^2\text{H}(e, e'\pi^-/\pi^+)X$, at $Q^2=0.5$ and $Q^2=1.0$ GeV^{29,30} from the Daresbury synchrotron. At the same time we also want to measure the exclusive reaction ${}^2\text{H}(e, e'p\pi^-)p_s$ to check whether measurement of the semi-exclusive reaction ${}^2\text{H}(e, e'\pi^-)pp_s$ gives a true account of the $n(e, e'\pi^-)p$ process. Exclusive measurements of this type have never been done before.

In all channels the neutron target measurements will cover the four momentum transfer range

$$0.2 \leq Q^2 \leq 3\text{GeV}^2 \quad .$$

III.3 Accidental Coincidences.

If all events are recorded which have an electron at scattering angles above 10° , then the inclusive electron rate about 100 sec^{-1} for a luminosity of $L = 10^{34} \text{ cm}^{-2} \text{ sec}^{-1}$. Accidentals may arise from two overlapping events, where in one event the electron is not detected. Since we require a hit in the CLAS scintillators for a charged particle to be accepted, the relevant time is the time resolution of the scintillator. With a (conservative) assumption of 2 nsec for the time resolution we obtain

$$\begin{aligned} N_c/N_e &\simeq 2 \cdot N_h \Delta\tau_{sc}, \\ &= 2 \cdot 1.5 \cdot 10^6 \cdot 2 \cdot 10^{-9} \\ &= 6 \cdot 10^{-3} \end{aligned}$$

where N_c is the accidental rate, N_e the electron rate, N_h is the total hadronic

interaction rate, and $\Delta\tau_{sc}$ the scintillator time resolution.

Although the accidental rate is already very low, it can be further reduced by requiring that the missing mass of the reconstructed event falls inside a very narrow missing mass bin around the pion or nucleon mass. This is extremely unlikely for uncorrelated particles. Under the assumed conditions accidentals will be completely negligible.

IV. Sensitivity to E_{1+}/M_{1+} and S_{1+}/M_{1+} .

The sensitivity of the coincidence cross section to the E_{1+} , S_{1+} , and M_{1+} multipoles can be best seen in the multipole decomposition of the single pion production cross section. In the approximation that only s waves and p waves with $J \leq 3/2$ contribute (a reasonable assumption near the maximum of the $\Delta(1232)$), and that the M_{1+} multipole dominates, the unpolarized cross section is given by:

$$\begin{aligned} d\sigma/d\Omega \simeq & \left[5/2|M_{1+}|^2 - 3\text{Re}(M_{1+}E_{1+}^*) + \text{Re}(M_{1+}M_{1-}^*) \right] \\ & + \cos\theta^* [2\text{Re}(E_{0+}M_{1+}^*)] \\ & + \cos^2\theta^* [-3/2|M_{1+}|^2 + 9\text{Re}(M_{1+}E_{1+}^*) - 3\text{Re}(M_{1-}M_{1+}^*)] \\ & + \epsilon \sin^2\theta^* \cos 2\phi [-3/2|M_{1+}|^2 - 3\text{Re}(M_{1+}E_{1+}^*)] \\ & + \sqrt{2\epsilon_L(\epsilon+1)} \sin\theta^* \cos\phi [-\text{Re}(S_{0+}M_{1+}^*) - 6\cos\theta^* \text{Re}(S_{1+}M_{1+}^*)] \end{aligned}$$

$$\epsilon_L = Q^2/(\vec{Q}^*)^2 \epsilon.$$

The sensitivity to E_{1+} and S_{1+} is in the interference terms with M_{1+} . In this approximation the terms

$$M_{1+}, \text{Re}(M_{1+}E_{1+}^*), \text{Re}(M_{1+}S_{1+}^*),$$

$$\text{Re}(E_{0+}M_{1+}^*), \text{Re}(S_{0+}M_{1+}^*), \text{ and } \text{Re}(M_{1-}M_{1+}^*)$$

can be uniquely determined by measuring the ϕ , and θ^* dependence of the cross section.

To study the sensitivity of the cross section measurement to the resonant multipoles without making use of the above assumptions, we used the results of an analysis of the world data at $Q^2=1 \text{ GeV}^2$ by Kroesen³¹. This analysis contained the resonant contributions up to F-waves and total angular momentum $J \leq 7/2$, as well as the nonresonant Born terms, and additional phenomenological background. The fit to the data is quite good, and the results should give a fairly realistic picture of the various contributions in the $\Delta(1232)$ region.

Figure 13 displays the various structure functions for $E_{1+}=0$, and for $E_{1+}/M_{1+} = 0.02$. σ_u and σ_{TT} are particularly sensitive to E_{1+} . The way that the multipoles can be determined from the measured cross section becomes more transparent in Figure 14 and Figure 15, where the cross section for the $p\pi^0$ channel is displayed for different azimuthal angles, and with

$$\begin{aligned} E_{1+} &= 0, & E_{1+}/M_{1+} &= 0.02 \\ \delta M_{1+} &= 0, & \delta M_{1+}/M_{1+} &= 0.05. \end{aligned}$$

The cross section at $\phi = 90^\circ$ is practically unaffected by E_{1+} , whereas it is strongly dependent on the value of M_{1+} . In the final analysis, the multipoles will be determined more precisely by a fit that takes into account all ϕ and θ values. In Figure 16 the expected error bars are superimposed on the Kroesen analysis results for different Q^2 . Since we do not know the precise Q^2 dependence of the various multipoles, we have assumed that all multipoles have the same Q^2 dependence. This, of course, is an over simplified assumption, and certainly not correct (e.g. we know that the resonant and nonresonant contribution to the inclusive cross section show a different Q^2 dependence). However, for demonstrating the statistical significance of the measurement it may still be useful. Note that this is the expected statistical accuracy for one θ bin of $\Delta\theta = 18^\circ$, and one W bin of $\Delta W = 20$ MeV. Near the maximum of the cross section the error bar for one $\Delta\cos\theta$ bin corresponds to an uncertainty

$$\begin{aligned} \delta E_{1+}/M_{1+} &\simeq 0.006 & \text{at } Q^2 &= 1.1\text{GeV}^2, \\ \delta E_{1+}/M_{1+} &\simeq 0.020 & \text{at } Q^2 &= 2.75\text{GeV}^2. \end{aligned}$$

In the extraction of the various multipoles we would use a global fit that takes into account the complete θ and ϕ information. We have estimated the statistical uncertainty of such a fit to be

$$\begin{aligned} \delta E_{1+}/M_{1+} &< 0.0015 & \text{at } Q^2 &= 1.1\text{GeV}^2, \\ \delta E_{1+}/M_{1+} &< 0.0050 & \text{at } Q^2 &= 2.75\text{GeV}^2. \end{aligned}$$

The proposed experiment would provide data with more than an order of magnitude improved statistical sensitivity over previous experiments. In Figure 17 the statistical errors for extraction of $Re(E_{1+}M_{1+}^*)/|M_{1+}|^2$ are displayed for different values of Q^2 .

Figure 18 - 19 shows the cross section for the π^+n channel. The shape of the cross section is significantly different from the π^0p channel due to the reduced resonant part ($\Delta(1232) \rightarrow p\pi^0 : \pi^+n=2:1$), and the increased nonresonant contributions in the forward direction (pion pole term). The sensitivity to the resonant multipoles, however, remains still strong.

In the final analysis, the data will be subjected to a detailed partial-wave analysis which fits the various isospin channels simultaneously, to obtain a nearly model independent determination of the various multipoles. For this analysis general theoretical principles (analyticity, unitarity) will help constrain the fit. These methods have been used very successfully in the analysis of pion photo-production data, and to some degree also in electroproduction³⁷. We refer here to the literature for a detailed discussion of these methods³⁸. We also anticipate that further progress in this area will be made, in particular a theoretical study of the nonresonant contributions at high Q^2 could prove very beneficial for this program.

Control of Systematic Errors.

With the proposed experimental program we will achieve a statistical precision of the data that need to be matched by a correspondingly precise control of systematic errors. In particular, since data measured with different parts of the detector will have to be combined and analyzed according to their θ and ϕ^* dependence a detailed understanding of the detector acceptance is necessary.

The CLAS detector offers a number of ways to control systematic uncertainties, which are usually not available when measurements of this type are performed with two separate magnetic spectrometers with small acceptance, and the spectrometers have to be moved to reach different kinematics.

- (1) The full kinematics is measured at one fixed setting therefore eliminating systematic uncertainties related to time dependent factors, like beam energy, charge integration, beam position and angle at the target, etc..
- (2) Elastic $ep \rightarrow ep$ scattering can be measured simultaneously with the normal data taking. Since the elastic cross section is known at the few percent level this process allows a precise calibration of the acceptances.
- (3) In addition to the elastic process we can measure the inclusive inelastic electron flux. Since the inclusive cross section is known very precisely, it can be used to establish the absolute cross section. It will also allow a very precise check of the detector uniformity.
- (4) The missing mass distribution in the reactions $p(e,e'p)\pi^0$, $p(e,e'p)\eta$, and $p(e,e'\pi^+)n$, can be used to calibrate angle and momentum reconstruction for charged tracks.
- (5) Measurement of the full ϕ distribution in single pion production rather than only a few ϕ points, allows an excellent control of the uniformity of the detector response. The parametrization

$$d\sigma/d\Omega = A + B \cos \phi + C \cos(2\phi)$$

with A, B, C independent of ϕ , must give a perfect fit to the measured cross section. This feature is of particular importance for the proposed program,

since a comparison of the pion production cross section at different ϕ angles is necessary to extract the electromagnetic multipoles.

- (6) Measurement of $p(e,e'p)\eta$ in the $S_{11}(1535)$ region allows a precise test of the ϕ uniformity of the detector response. Previous measurements have shown that the η production is dominated (to more than 90%) by s-wave production. Note that the s-wave part of the cross section has no ϕ dependence. In an analysis of the partial wave composition of η production, the s-wave part of the cross section must be independent of ϕ .

We believe that combining several of these checks will enable us to control the systematic uncertainties of the measurement at the required level.

V. Requirement.

V.1. Beam Time

For the initial measurement we request 1000 hrs of beam time with a hydrogen target, and 100 hrs with a deuterium target. The beam energy will be 4 GeV. To cover the low Q^2 range we request an additional 300 hours for each target at 2 GeV beam energy. We note that the data can be accumulated together with data covered by other proposals of the N^* group.

V.2. Trigger.

Data would be taken initially with an electron trigger only, where we require a minimum energy deposition in the calorimeter, and hits in the Cerenkov counters and scintillation counters that geometrically match with the calorimeter signal. We have estimated the total trigger rate (including elastic events) for such a trigger using the CELEG and FASTMC simulation packages, as shown in Figure 4 of part A.III. We believe that this rate can be accepted by the data acquisition scheme presently under development for the CLAS detector.

Provided that a reliable, more sophisticated trigger scheme is operational, allowing selection of more restrictive event patterns, we would require an additional charged particle anywhere in the detector. Such a trigger would not reduce the true event rate significantly, however, it would largely eliminate false triggers from cosmic rays and particles backscattered from the beam dump.

V.3. Targets.

The experiment will need a low power target, either of liquid hydrogen (deuterium) or of pressurized hydrogen gas. We are looking into the possibility to employ a narrow Kapton cell, where the side walls are reinforced with a wire

structure. The entrance windows would have a very small diameter (a few millimeters), making use of the small beam spot size of the CEBAF accelerator. The entrance and exit windows could then be made of thin (e.g. $5\mu\text{m}$) capton foils or other low Z material. For a 10 cm long gas volume at 10 atm pressure a beam current of $0.32\mu\text{A}$ is needed to achieve $10^{34}\text{cm}^{-2}\text{sec}^{-1}$ luminosity.

VI. Future Polarization Measurements.

We plan to continue this effort with additional polarization experiments. Measurement of the electron asymmetry using a polarized electron beam allows the measurement of the "fifth structure function", which is sensitive to interferences between resonant and nonresonant amplitudes. In the region of the $\Delta(1232)$ the terms

$$\text{Im}(S_{0+}M_{1+}^*), \text{ and } \text{Im}(S_{1+}M_{1+}^*)$$

can be determined. Experiments employing polarized targets allow the measurement of 8 additional structure functions. Not all of these structure functions may be important to measure. In the $\Delta(1232)$ region, however, one can determine the corresponding "missing" imaginary parts of those terms whose real parts are measured in unpolarized experiments. These are

$$\text{Im}(E_{1+}M_{1+}^*), \text{ and } \text{Im}(M_{1-}M_{1+}^*) .$$

With such a complete set of information on the bilinear multipole products in the $\Delta(1232)$ region a nearly model-independent determination of the magnitude and phases of the multipoles should be feasible.

VII. Summary.

We have proposed a high statistics measurement of pion electroproduction in the region of the $\Delta(1232)$ resonance. The data obtained in this measurement will allow a precise determination of the electric quadrupole multipoles E_{1+} , the scalar multipole S_{1+} , and the magnetic multipole M_{1+} for a Q^2 range of 0.2 to 3.0 GeV^2 . Additional information will be obtained on the (nonresonant) M_{1-} and S_{0+} multipoles. This information will allow precise tests of microscopic models of baryon structure. In Table VII.1 the requirements are summarized,

Table VII.1 Summary of Requirements

Energy (GeV)	Target	Beam Time (hrs)	Luminosity ($\text{cm}^{-2}\text{sec}^{-1}$)	CLAS-Field
4	H_2	1000	$\simeq 10^{34}$	B_o
	D_2	1000	$\simeq 10^{34}$	B_o
2	H_2	300	$\simeq 3 \cdot 10^{33}$	$0.5 \cdot B_o$
	D_2	300	$\simeq 3 \cdot 10^{33}$	$0.4 \cdot B_o$

References.

- [1] Proceedings of the International Workshop on "Excited Baryons 1988", August 4-6, 1989, Troy, NY; eds. G. Adams, N.C. Mukhopadhyay, and P. Stoler.
- [2] R. Davidson, N.C. Mukhopadhyay, R. Wittman; Phys. Rev. Lett. 56, 804(1986).
- [3] M. Bourdeau, N.C. Mukhopadhyay; Phys. Rev. Lett. 58, 976(1987).
- [4] C.E. Carlson; Phys. Rev. D34, 2704(1986).
- [5] K. Bermuth, D. Drechsel, L. Tiator, J.B. Seaborn; Phys. Rev. D37, 89(1989).
- [6] S. Kumano; Phys. Lett. 214, 132(1988).
- [7] E. Eich; Z. Phys. C 38, 399(1988).
- [8] F. Iachello; Phys. Rev. Lett. 62, 2704(1989).
- [9] M. Warns, H. Schroeder, W. Pfeil, H. Rollnik; BONN-ME-89-03(1989).
- [10] M. Warns, H. Schroeder, W. Pfeil, H. Rollnik; BONN-ME-89-04(1989).
- [11] F.E. Close, Z. Li; ORNL Preprint (1989).
- [12] W. Konen, H. Weber; Preprint MKPH-T-89-11/ UVa-INNPP-89-6(1989).
- [13] J.G. Koerner; Z. Phys. C 33, 529 (1987).
- [14] P. Christellin, G. Dillon; Preprint IPNO/TH 88-23(1988).
- [15] C.E. Carlson, J.L. Poor; Preprint WM-88-101(1988).
- [16] N. Isgur, G. Karl; Phys. Lett. 72B, 109(1977).
Phys. Rev. D23, 817(1981).
- [17] S. Ono; Nucl. Phys. B107, 522(1976).
- [18] F. Ravndal; Phys. Rev. D4, 1466(1971).
- [19] C. Carlson; in [1]
- [20] V.L. Chernyak, I.R. Zhinitsky; Nucl. Phys. B246, 52(1984).
- [21] I.D. King, C.T. Sachrajda; Nucl. Phys. B279, 785(1987).
- [22] M. Gari, N. Stefanis; Phys. Lett. B175, 462(1986).
- [23] K. Baetzner et al.; Nucl. Phys. B76, 1(1974).
- [24] W. Albrecht et al., Nucl. Phys. B25, 1(1970)
W. Albrecht et al.; Nucl. Phys. B27, 615(1971)
S. Galster et al.; Phys. Rev. D5, 519(1972)
R. Siddle et al., Nucl. Phys. B35, 93(1971)
R.D. Hellings, et al.; Nucl. Phys. B32, 179(1971)

- J.C. Alder et al.; Nucl. Phys. B46, 573(1972)
 K. Baetzner et al.; Nucl. Phys. B75, 1(1974).
- [25] G. v.Gehlen; (1971); Nucl. Phys. B26, 141(1971).
 [26] W. Brasse et al.; Nucl. Phys. B110, 410(1976).
 [27] D. Joyce; CLAS Note 89-004, unpublished.
 [28] E. Smith; CLAS Note 89-003, unpublished #
 [29] J. Wright et al.; Nucl. Phys. B181, 403(1981).
 [30] O. Vapenikova et al.; Z. Phys. C37, 251(1988).
 [31] G. Kroesen; Bonn IR-83-3(1983), unpublished.
 [32] R. Koniuk, N. Isgur; Phys. Rev. D21, 1868(1980).
 [33] F. Foster, G. Hughes; Rep. Prog. Phys. Vol46, 1445(1983).
 [34] S.A. Gogilidze et al.; Yad. Fiz. 45, 1085(1987).
 [35] E. Evangelides et al.; Nucl. Phys. B71, 381(1974)
 J.C. Alder et al.; Nucl. Phys. B99, 1(1975)
 H. Breuker et al.; Nucl. Phys. B146, 285(1978)
 H. Breuker et al.; Z. Phys. C13, 113(1982)
 H. Breuker et al.; Z. Phys. C17, 121(1983).
- [36] N. Isgur, C.H. Llewellyn-Smith; Nucl. Phys. B212, 526(1989).
 [37] R.C.E. Devenish, D.H. Lyth; Nucl. Phys. B93, 109(1975).
 [38] R.G. Moorhouse; Electromagnetic Interactions of Hadrons,
 Vol. 1, Plenum Press, New York and London,
 eds. A. Donnachie, G. Shaw.
- [39] C. Becchi, G. Mopurgo; Phys. Rev. 140, B687(1965)
 H. Harari, H. Lipkin; Phys. Rev. 140B, 1617(1965).
 [41] C. Papanicolas; in Ref. [1]

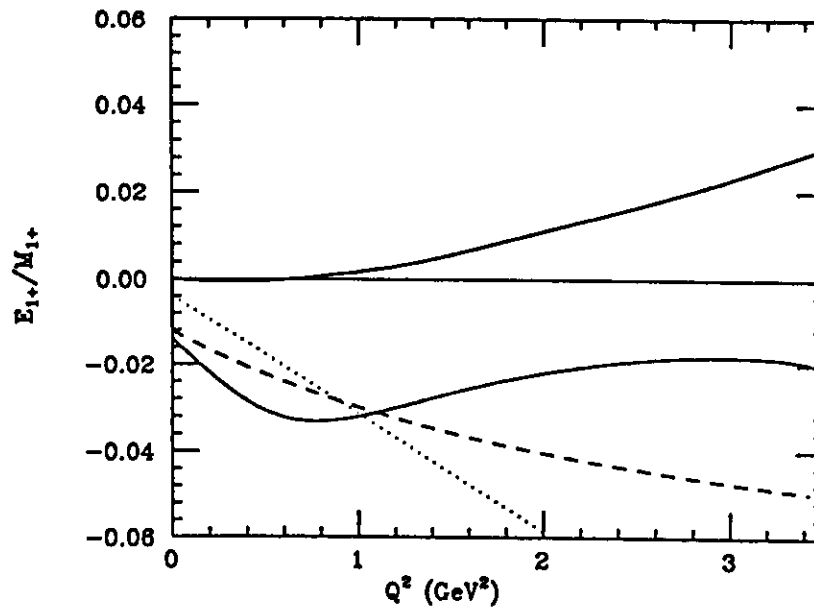
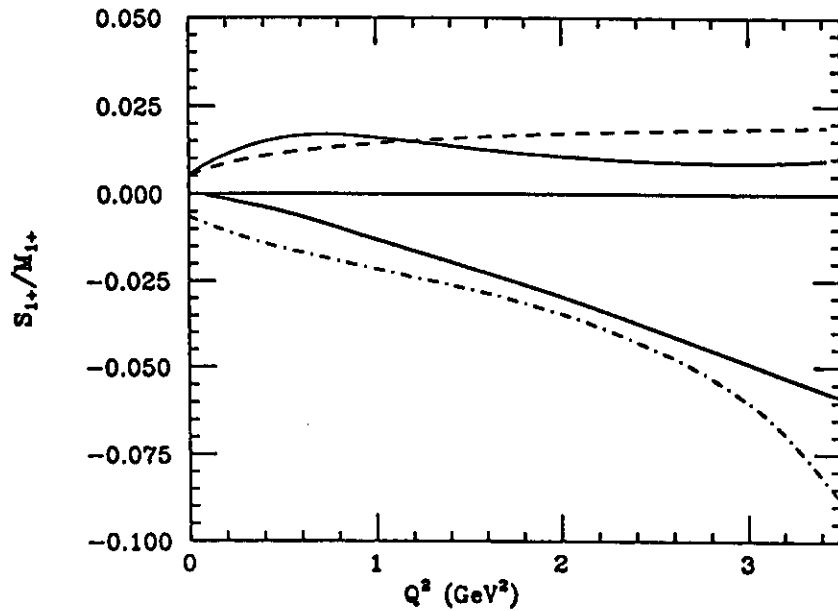


Figure 1. The E_{1+}/M_{1+} and S_{1+}/M_{1+} ratios versus Q^2 as predicted in the nonrelativistic quark model with configuration mixing¹⁶ (dashes line), the relativized quark model of Warns et al.¹⁶ (thin solid line), the non-relativistic quark model calculation of Gogilidze et al.^{3,4} (dotted line), and the Generalized Vector Dominance Model of Koerner¹³ (bold solid line).

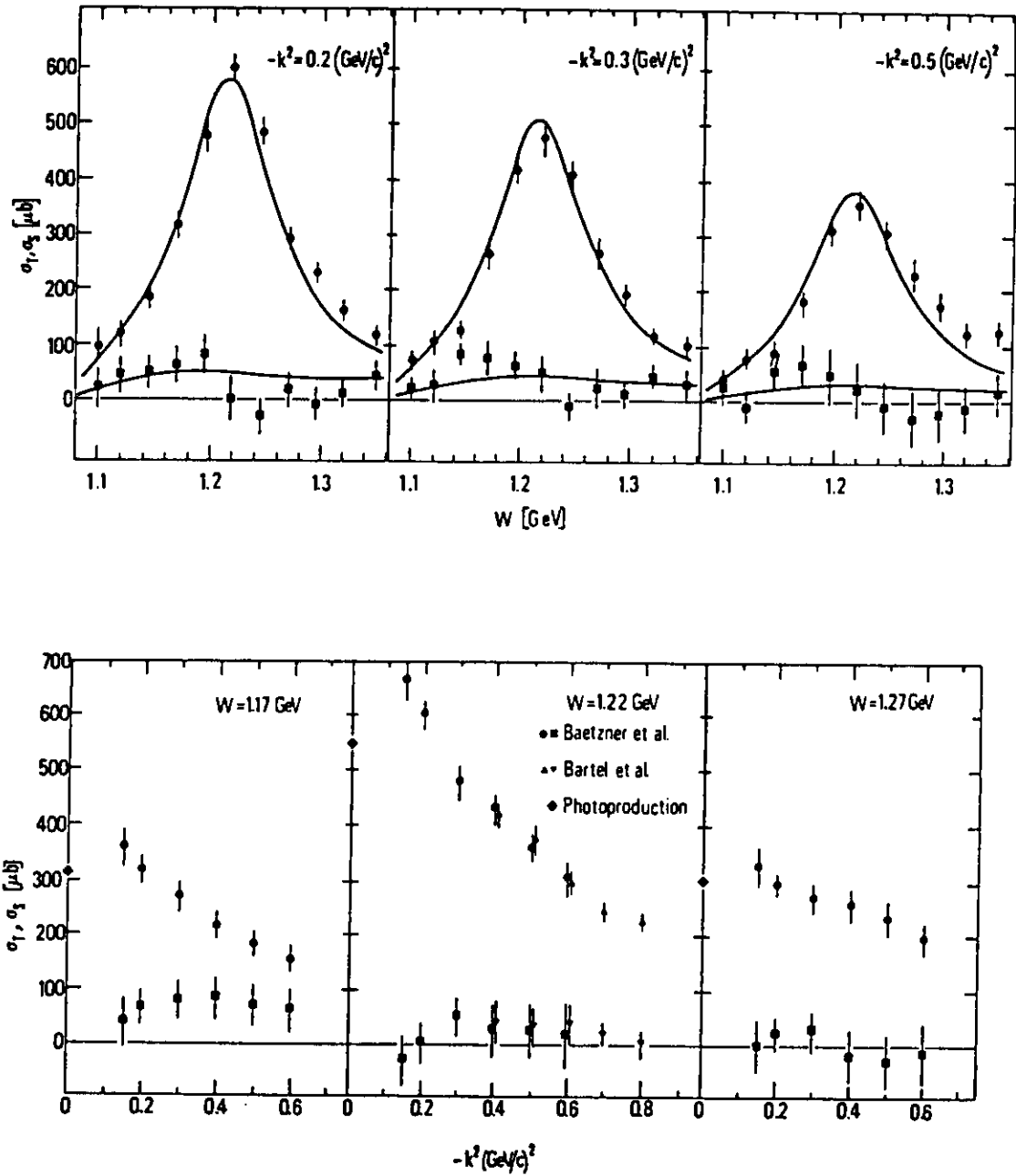


Figure 2. Separated values σ_T (full circles) and σ_L (squares) versus W at fixed four momentum transfer (top) and at fixed W (bottom) according to Baetzner et al.²³.

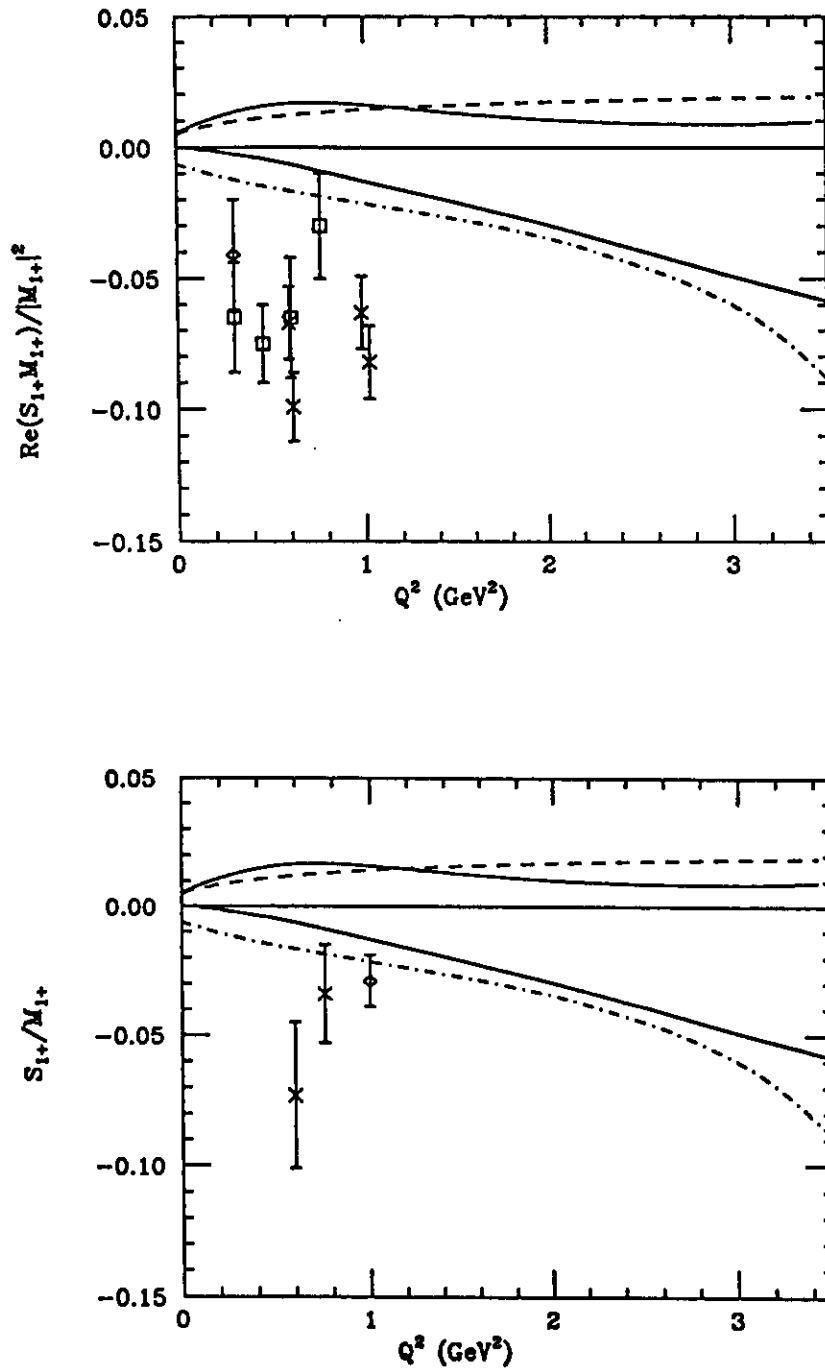


Figure 3. Comparison of experimental data on the interference term $\text{Re}(S_{1+} M_{1+}^*) / |M_{1+}|^2$ with theoretical predictions (same as in Figure 1). The data are from experiments performed at Bonn, DESY, and NINA²⁴. The S_{1+} / M_{1+} results have been obtained from a more detailed analysis.

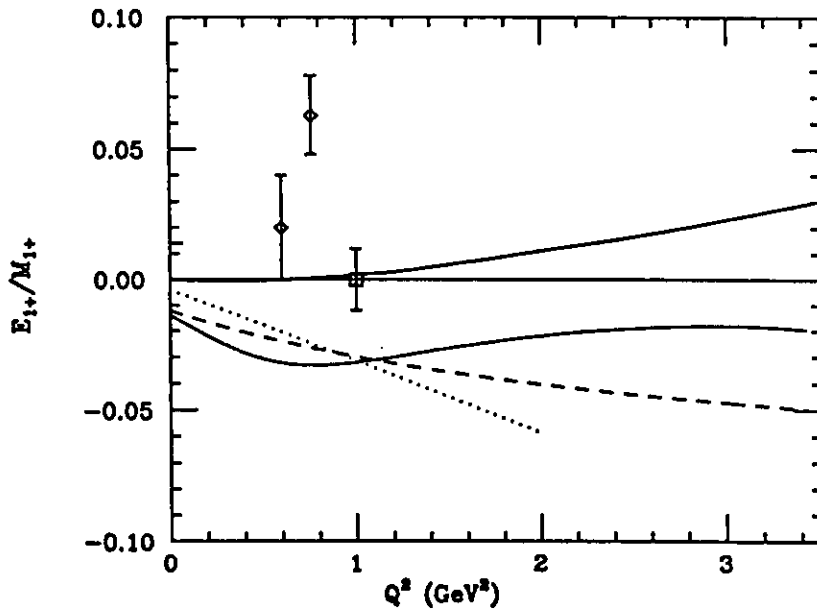
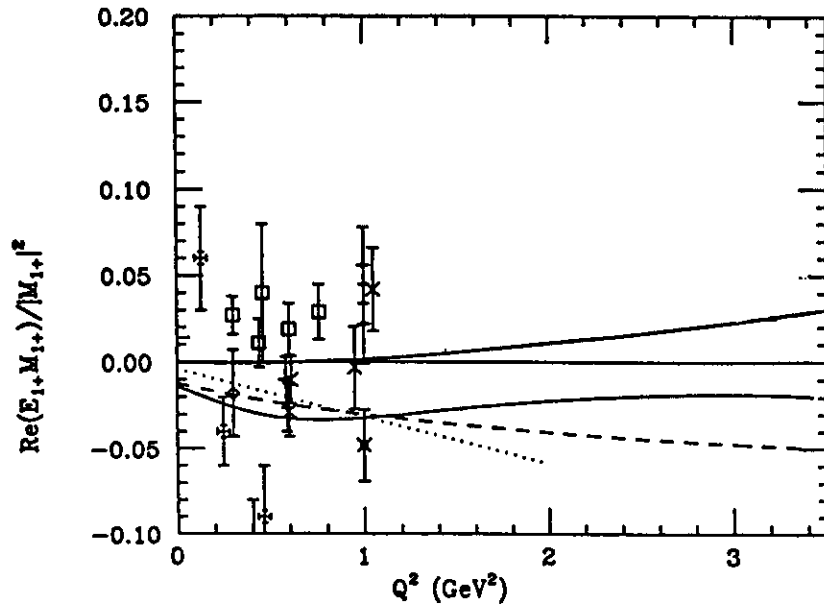


Figure 4. Comparison of experimental data²⁴ on the interference term $\text{Re}(E_{1+} M_{1+}^*) / |M_{1+}|^2$ with theoretical predictions. Same references as in Figure 3.

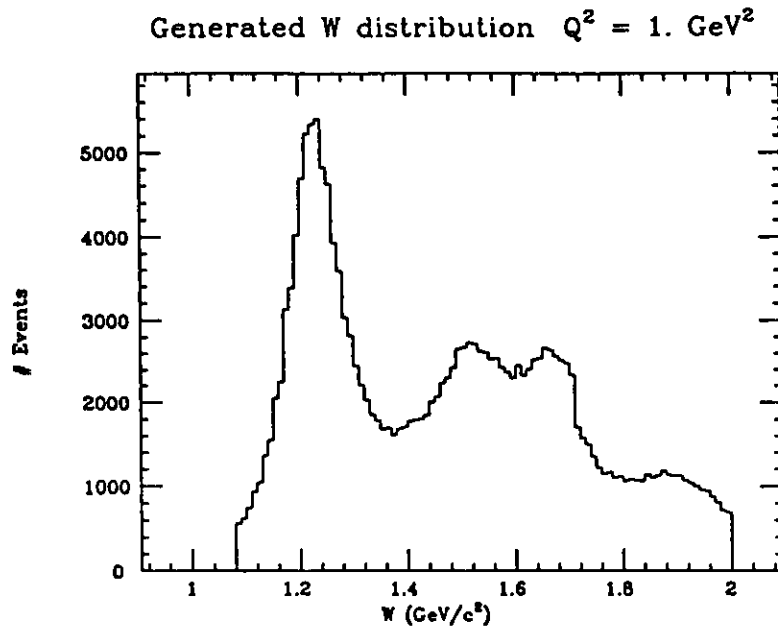


Figure 5. Invariant mass W distribution as generated by CELEG at $Q^2 = 1\text{GeV}^2$, with an incident beam energy of 4GeV (all resonances included).

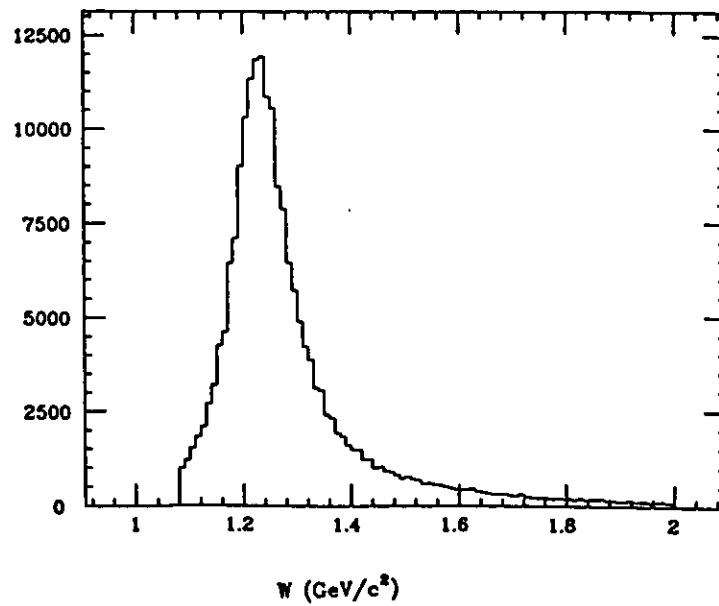
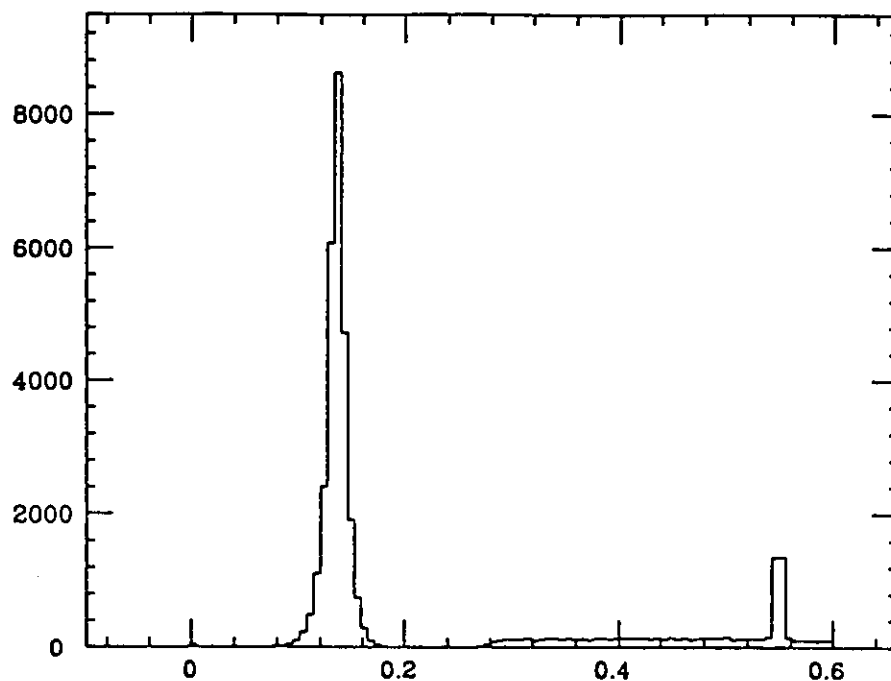


Figure 6. Same as in Figure 5, but only $\Delta(1232)$ resonance included.

missing mass - smeared



missing mass - smeared

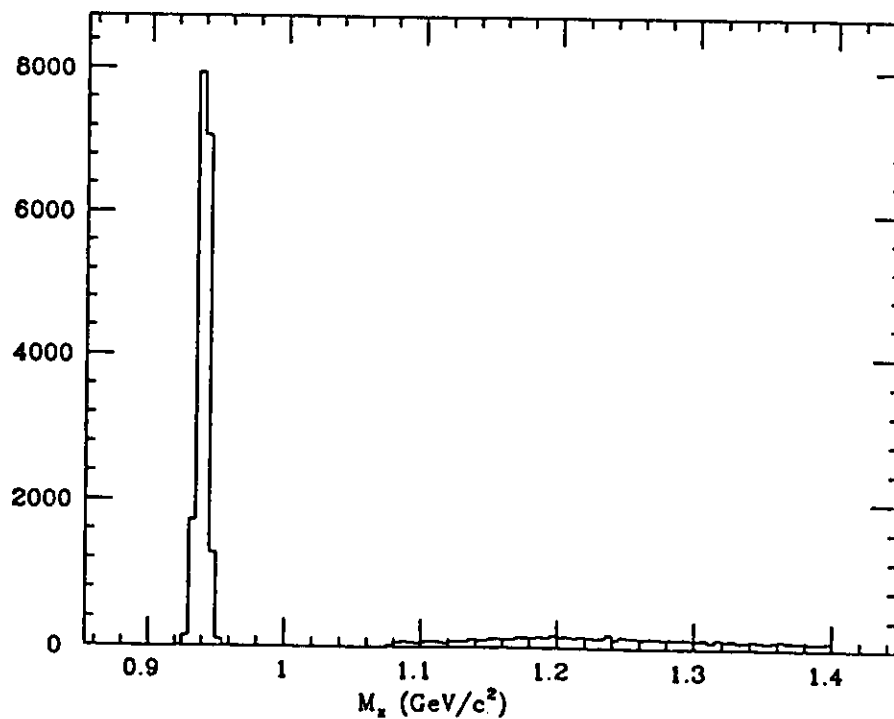


Figure 7. Missing mass distribution for the reactions $p(e,e'p)X$ and $p(e,e'\pi^+)X$ as generated by CELEG and FASTMC. Note that the $p\pi^0$ and $n\pi^+$ channels are well separated from the two-pion production threshold. All resonances were included in the simulation.

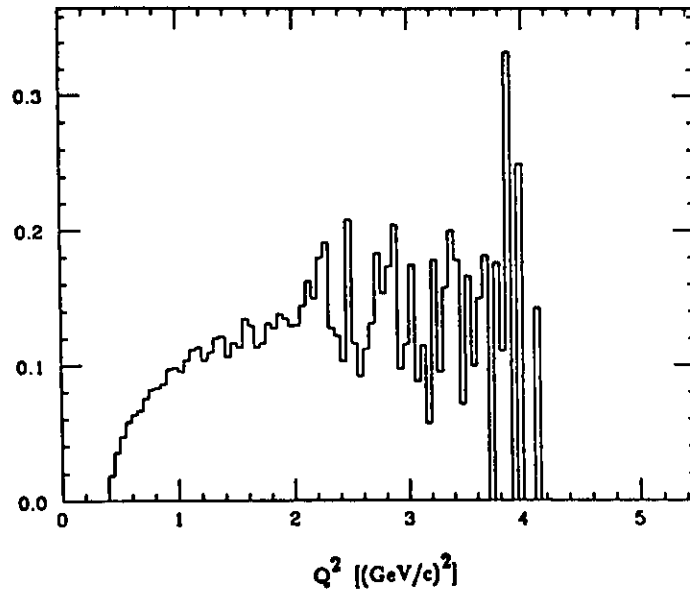
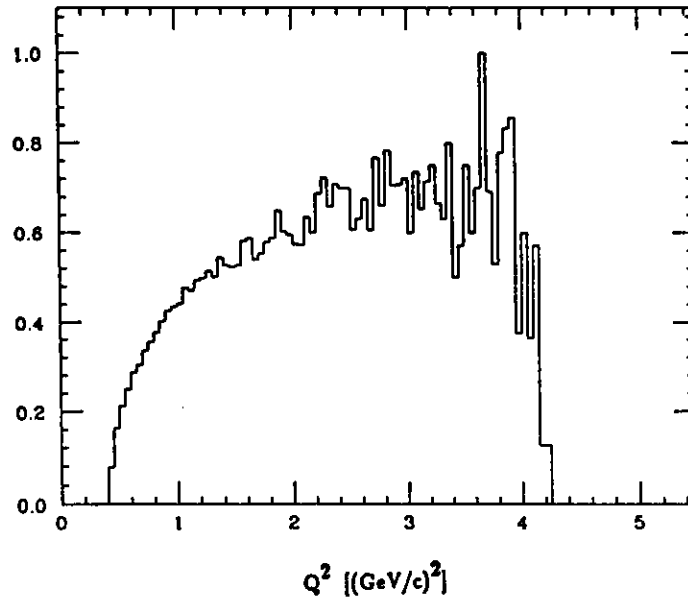


Figure 9. CLAS acceptance in Q^2 for $\Delta(1232)$ events. Top: (accepted e^-) / (generated e^-). Bottom: (accepted $e^- p \pi^0$) / (generated e^-).

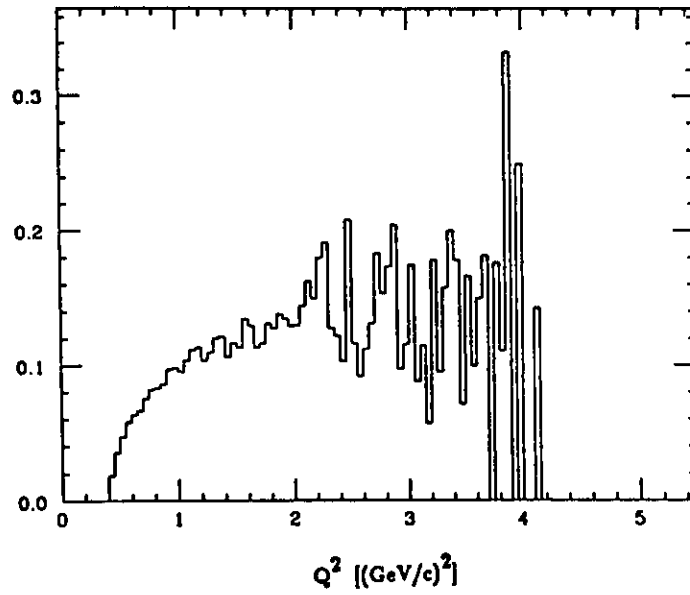
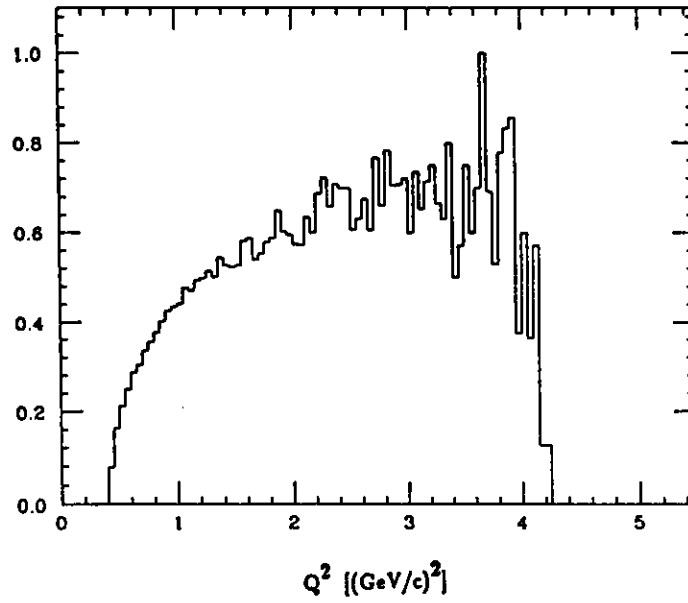


Figure 9. CLAS acceptance in Q^2 for $\Delta(1232)$ events. Top: (accepted e^-) / (generated e^-). Bottom: (accepted $e^- p^* \pi^0$) / (generated e^-).

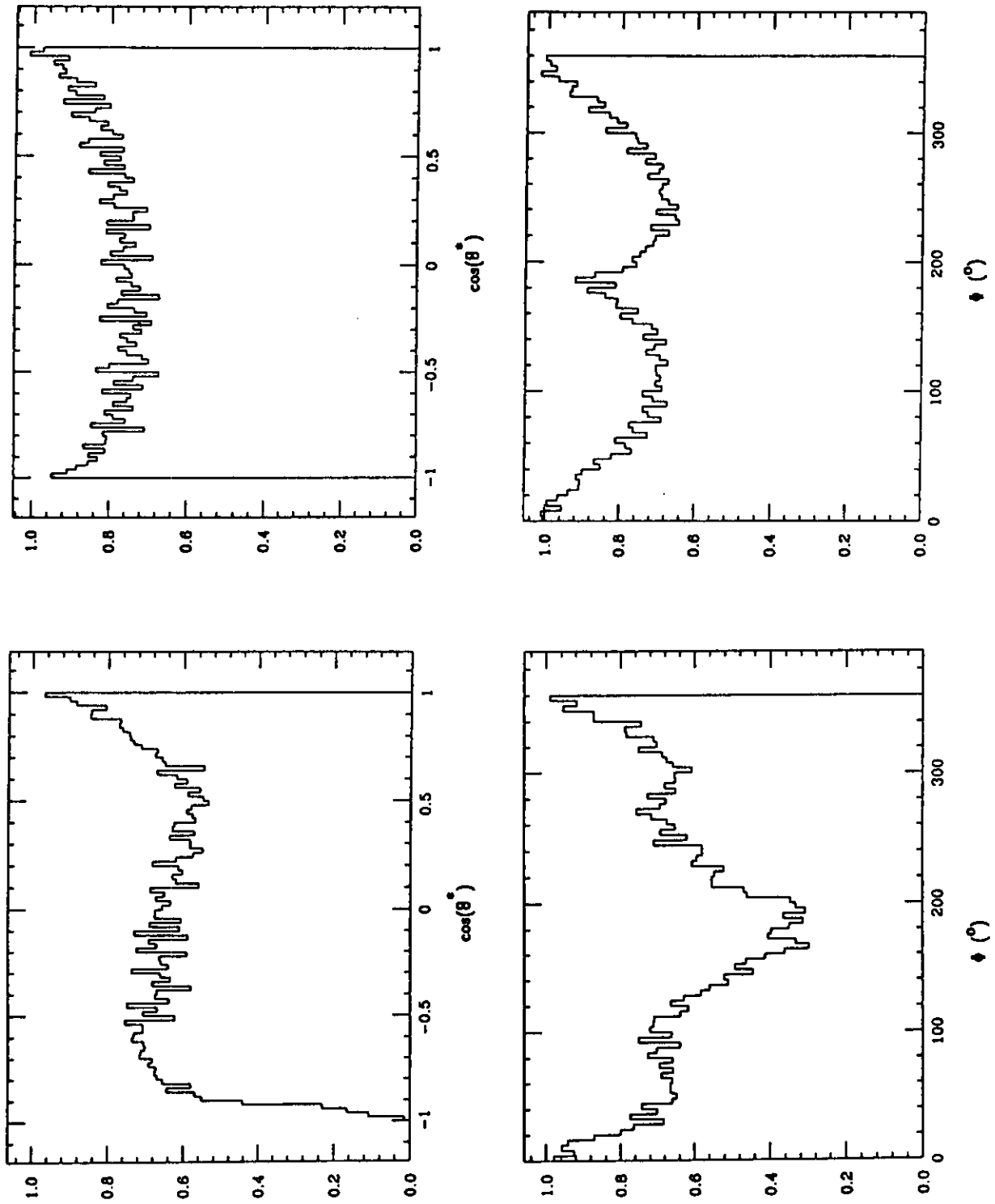


Figure 10. CLAS acceptance in the center-of-mass angles θ^* and ϕ of the $N\pi$ system for $\Delta(1232)$ events at $Q^2 = 1.0 \text{ GeV}^2$. Left: $\Delta \rightarrow p\pi^0$. Right: $\Delta \rightarrow n\pi^+$.

Electroproduction: π^0 at $Q^2=1.0 \text{ GeV}^2/c^2$

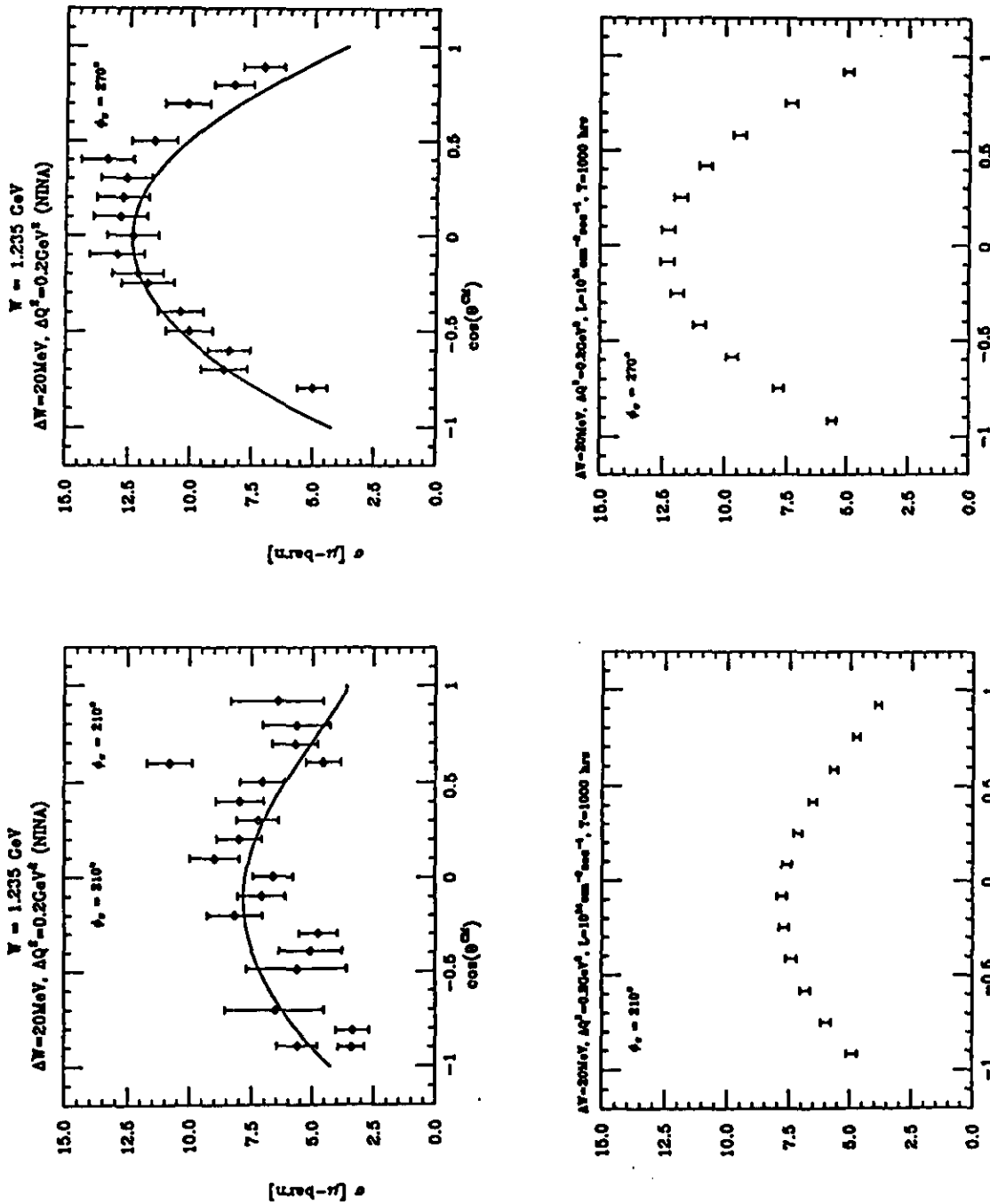


Figure 11. Comparison of statistical accuracy of existing data $p(e,e')\pi^0$ at $W=1.232\text{GeV}$, with statistical errors of data expected with CLAS. Running time is 1000 hrs, at a luminosity of $10^{34} \text{ cm}^{-2} \text{ sec}^{-1}$. Bin sizes in the experimental results and in the simulation are identical. The complete acceptance functions of CLAS have been folded in. The curves are the result of a phenomenological fit to the data. The curves were generated by the CLAS Monte Carlo program.

Electroproduction: π^0 at $Q^2=1.0 \text{ GeV}^2/c^2$

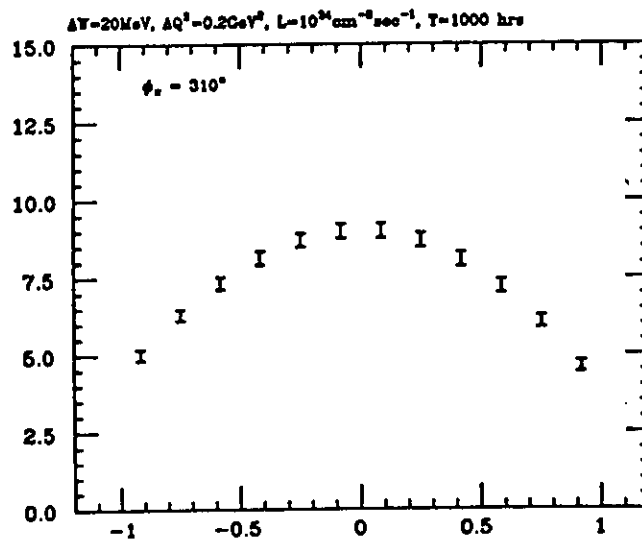
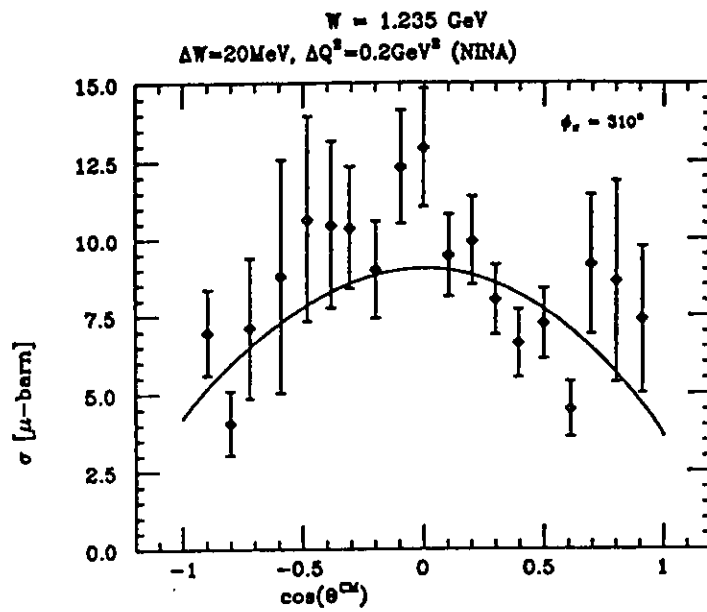


Figure 11. (continued)

Electroproduction: π^+ at $Q^2=1.0 \text{ GeV}^2/c^2$

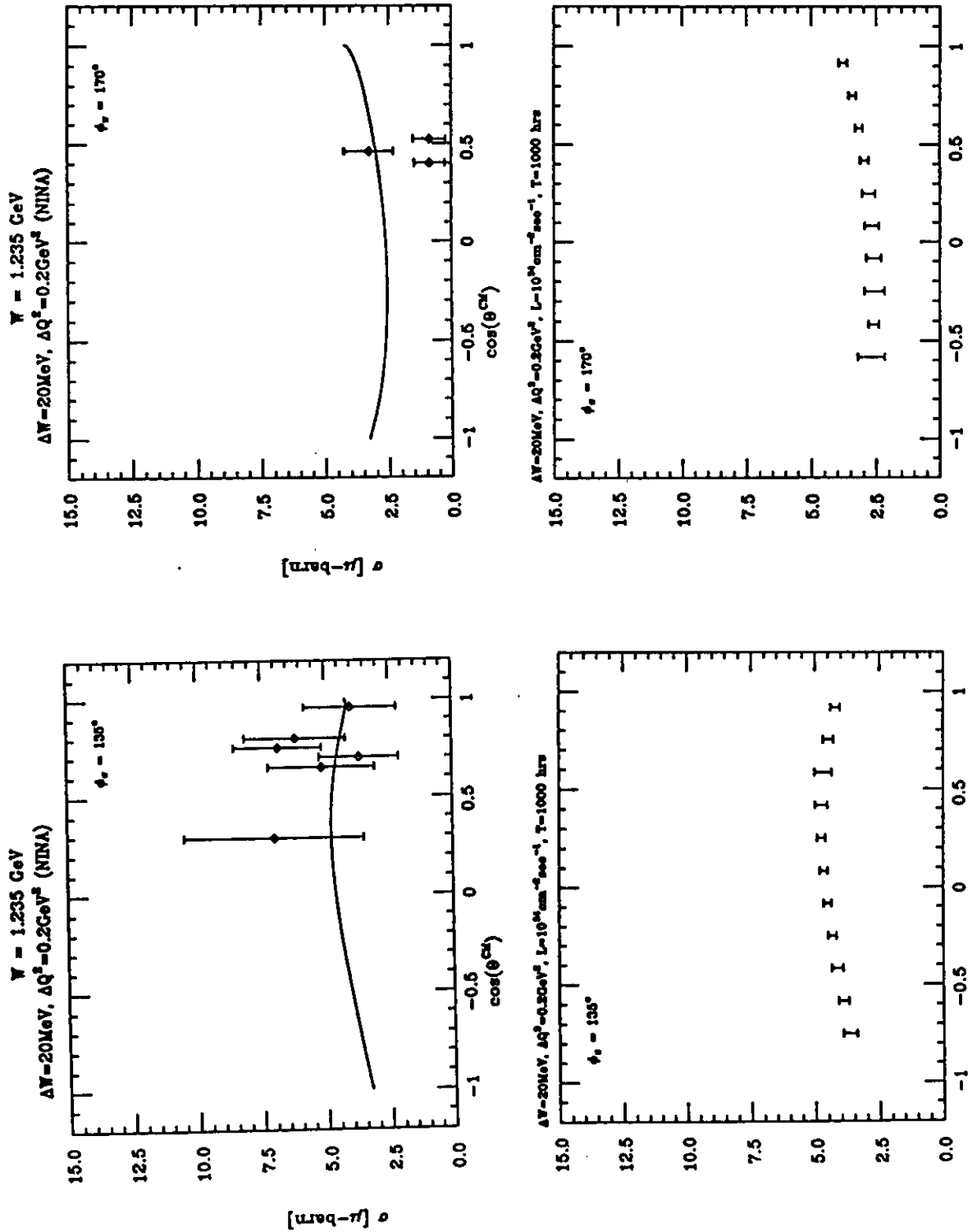


Figure 12. Same as in Figure 11, but for the $p(e,e'\pi^+)n$ channel.

Electroproduction: π^+ at $Q^2=1.0 \text{ GeV}^2/c^2$

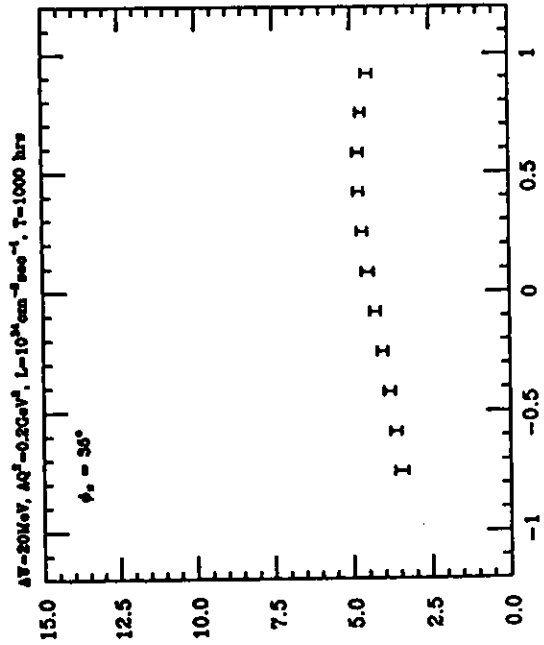
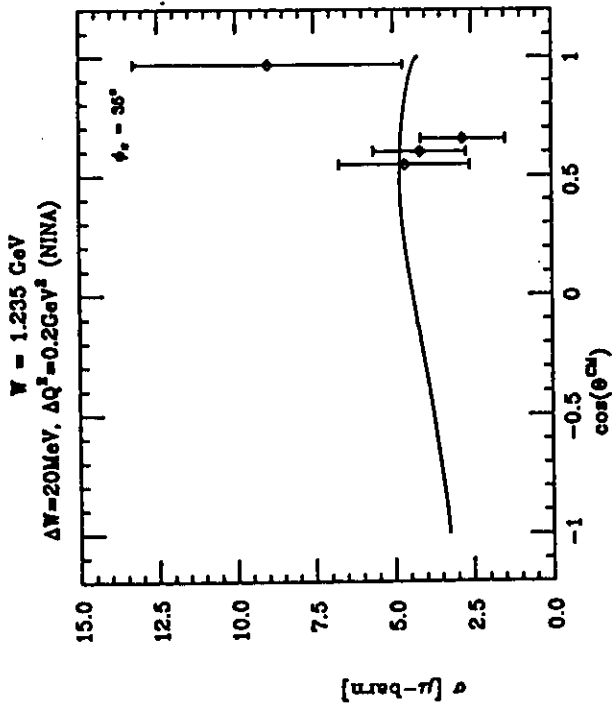
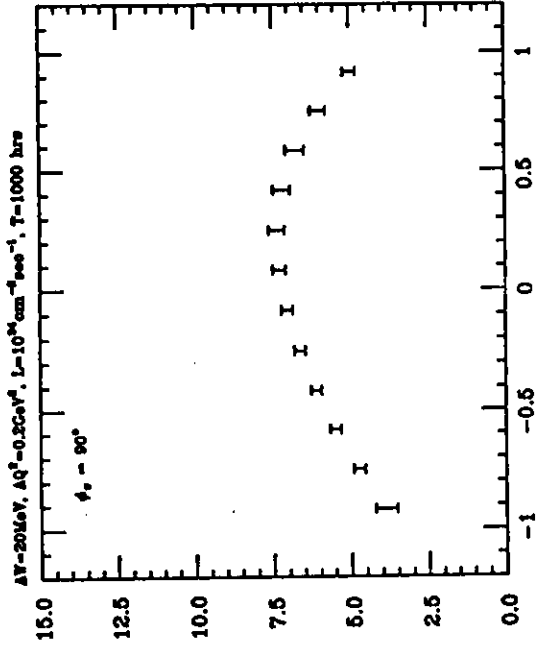
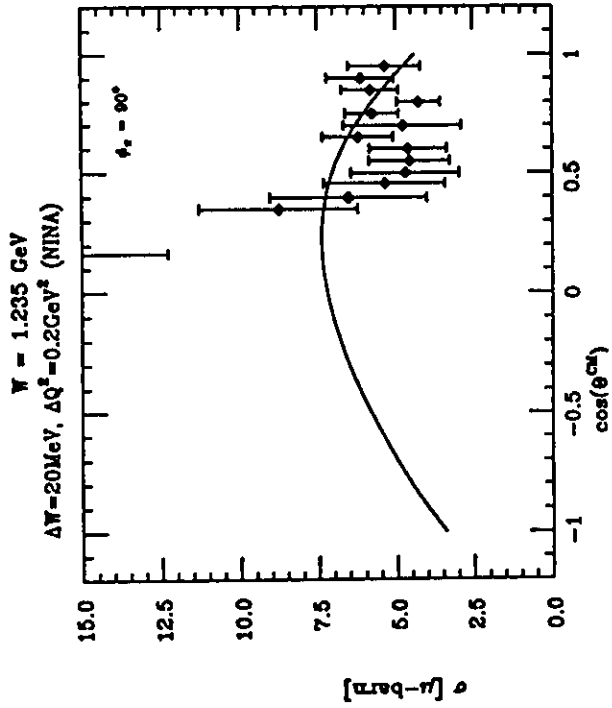


Figure 12 (continued).

Electroproduction: π^0 at $Q^2=1.0 \text{ GeV}^2/c^2$

$W = 1.232 \text{ GeV}$

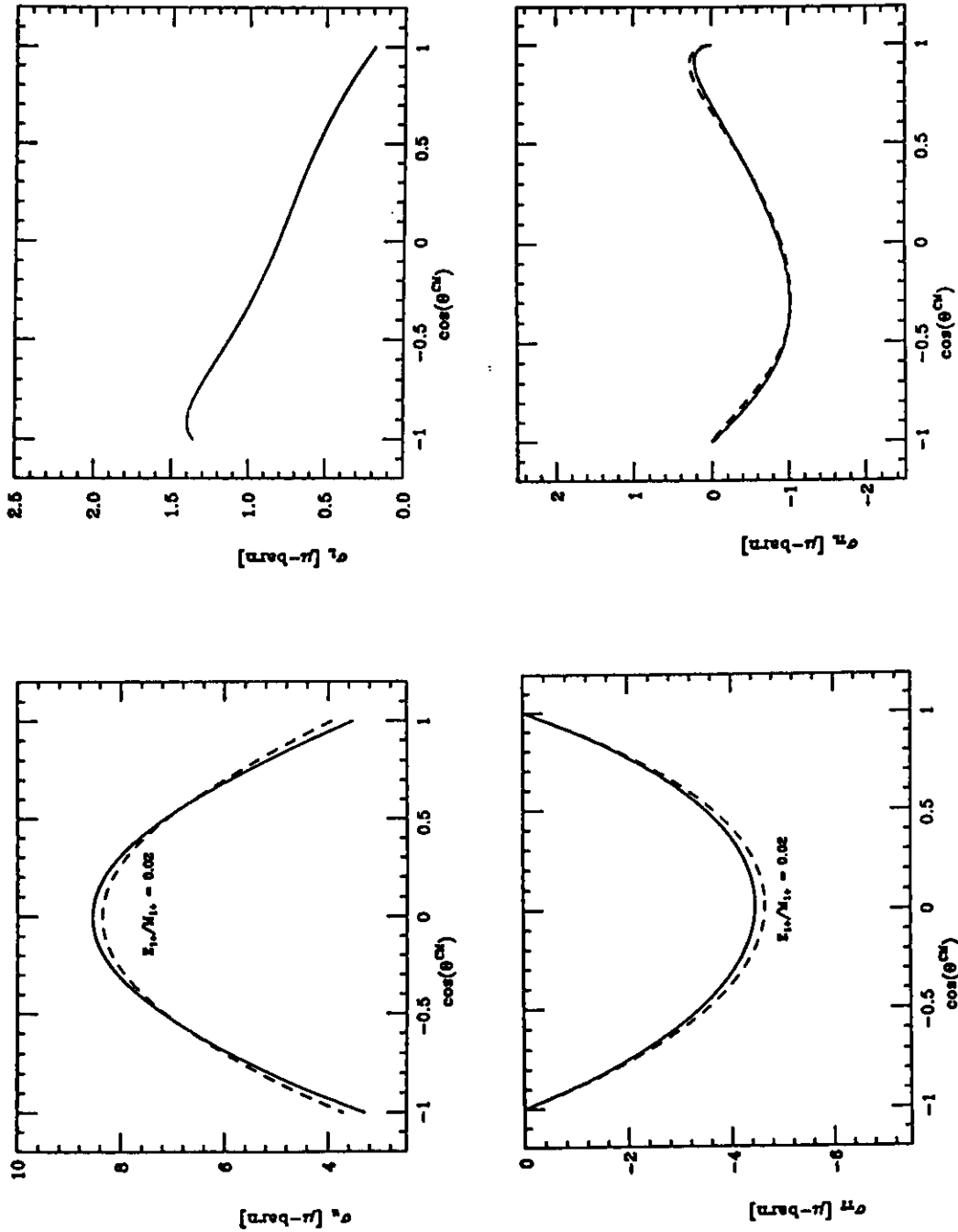


Figure 13. The structure functions σ_u , σ_L , σ_{TT} , and σ_{TL} for $p(e,e'p)\pi^0$ at $Q^2=1.0\text{GeV}$, for $E_{1+}=0$ (solid lines), and $E_{1+}/M_{1+}=0.02$ (dashed lines). σ_u and the interference term σ_{TT} are most sensitive to small variations of E_{1+} .

Electroproduction: π^0 at $Q^2=1.0 \text{ GeV}^2/c^2$

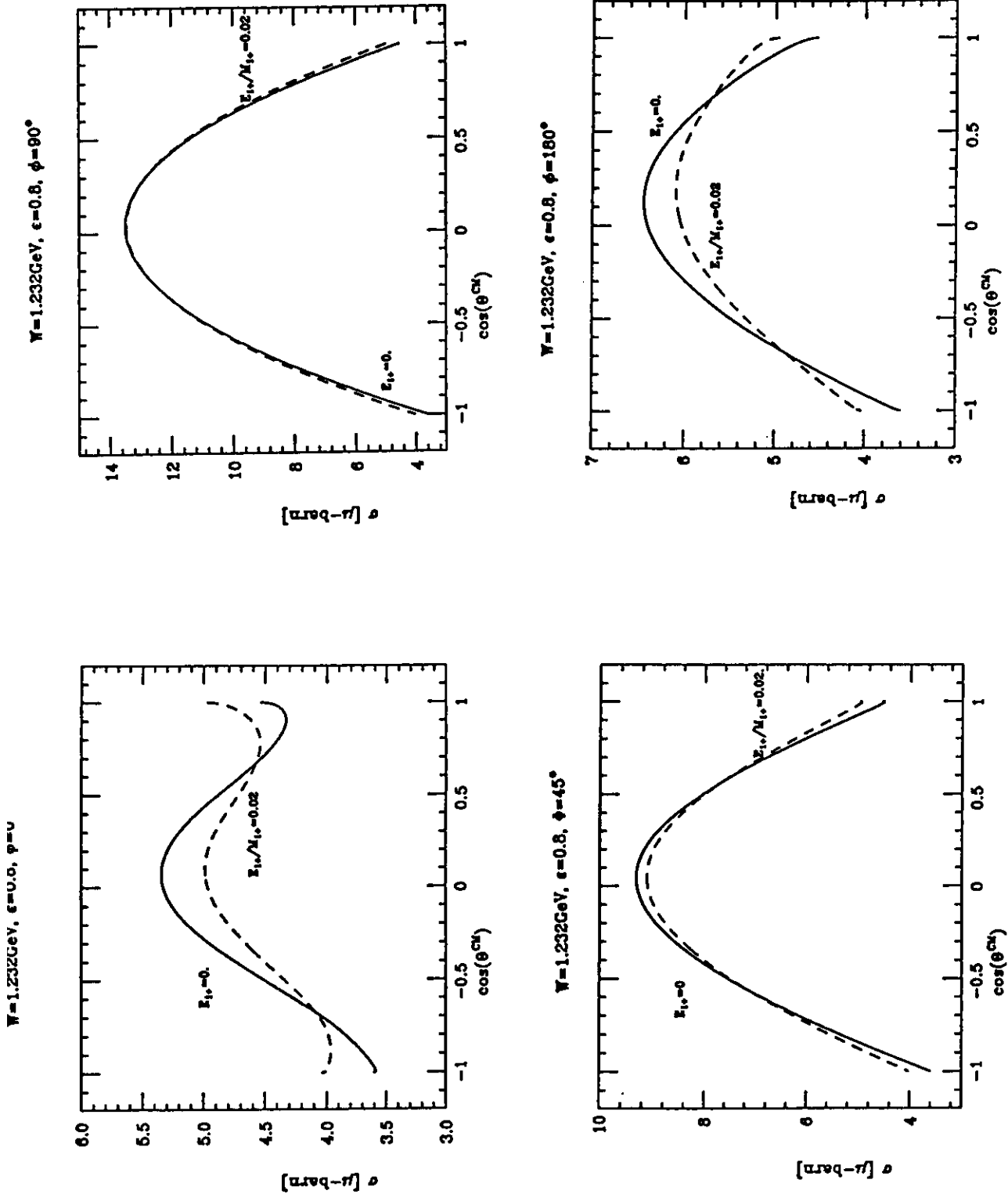


Figure 14. Angular distributions for $p(e,e'p)\pi^0$ at $Q^2=1.0 \text{ GeV}^2$ at various azimuthal angles ϕ , for $E_{1+}=0$, and $E_{1+}/M_{1+}=0.02$, respectively. Cross sections at $\phi=0$, and $\phi=180^\circ$ are most sensitive to E_{1+} contributions.

Electroproduction: π^0 at $Q^2=1.0 \text{ GeV}^2/c^2$

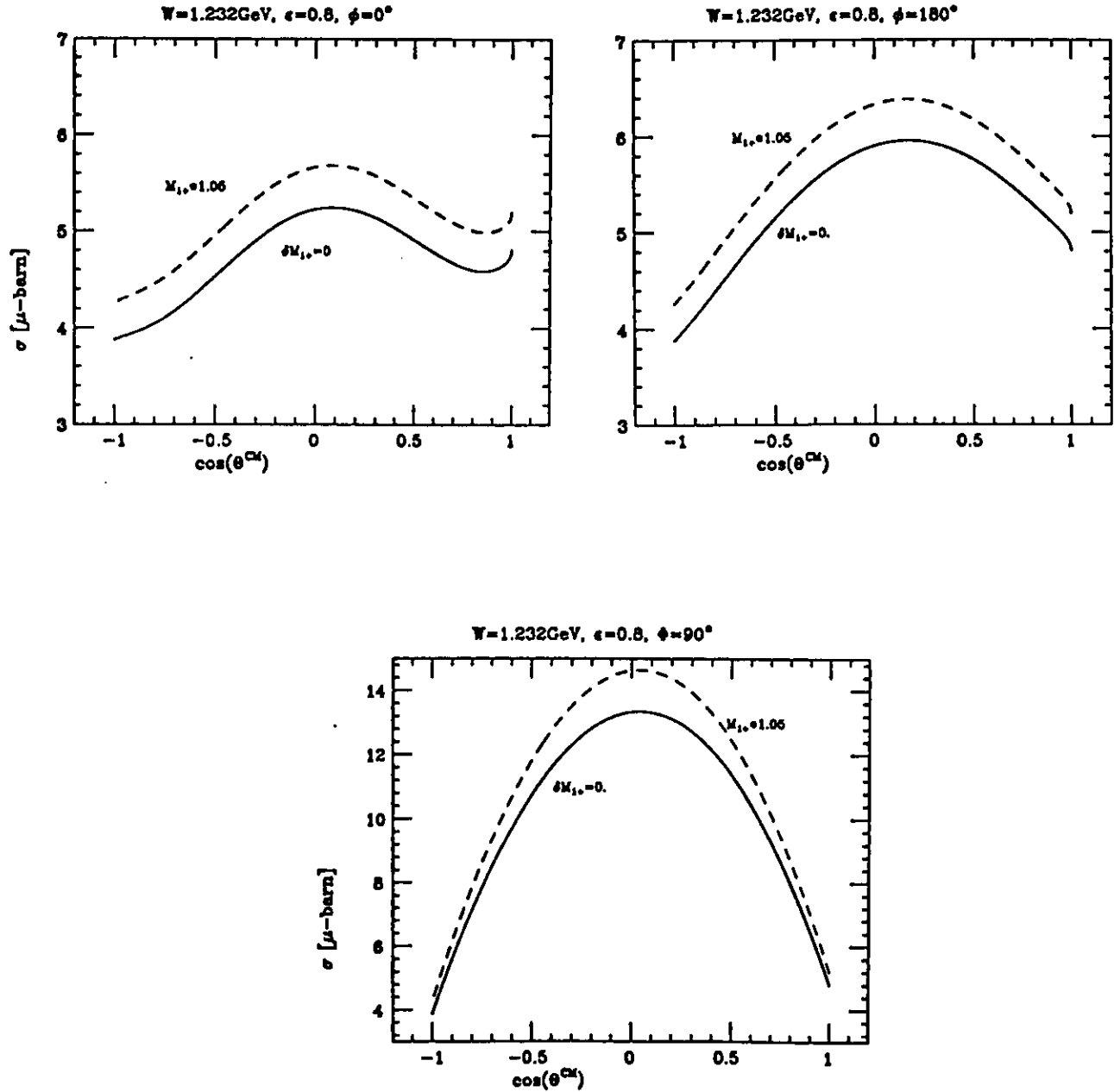


Figure 15. Same as in Figure 14, but for $\delta M_{1+}=0$, and $\delta M_{1+}/M_{1+}=0.05$.

$\epsilon=0.8, \phi=0^\circ, W=1.232\text{GeV}$

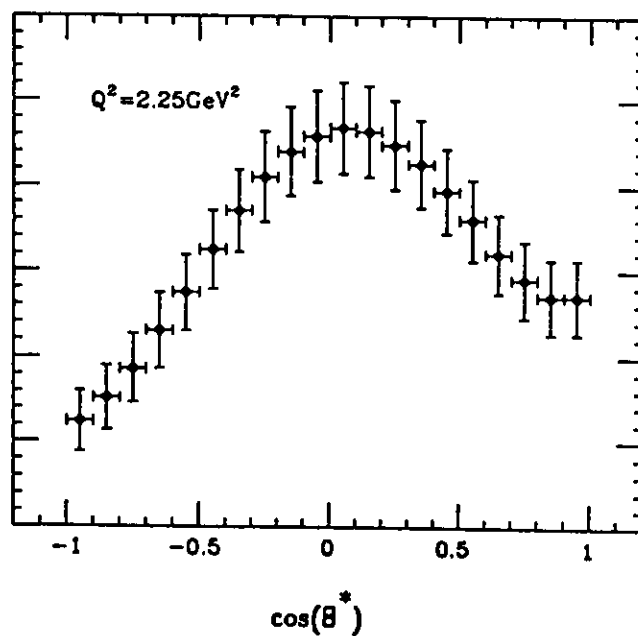
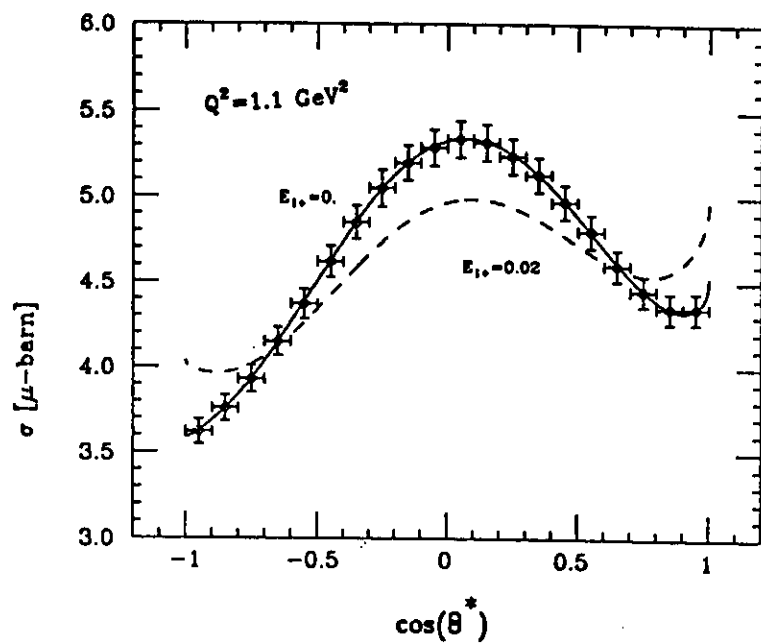


Figure 16. Expected statistical error bars of the $p\pi^0$ cross section measurement.

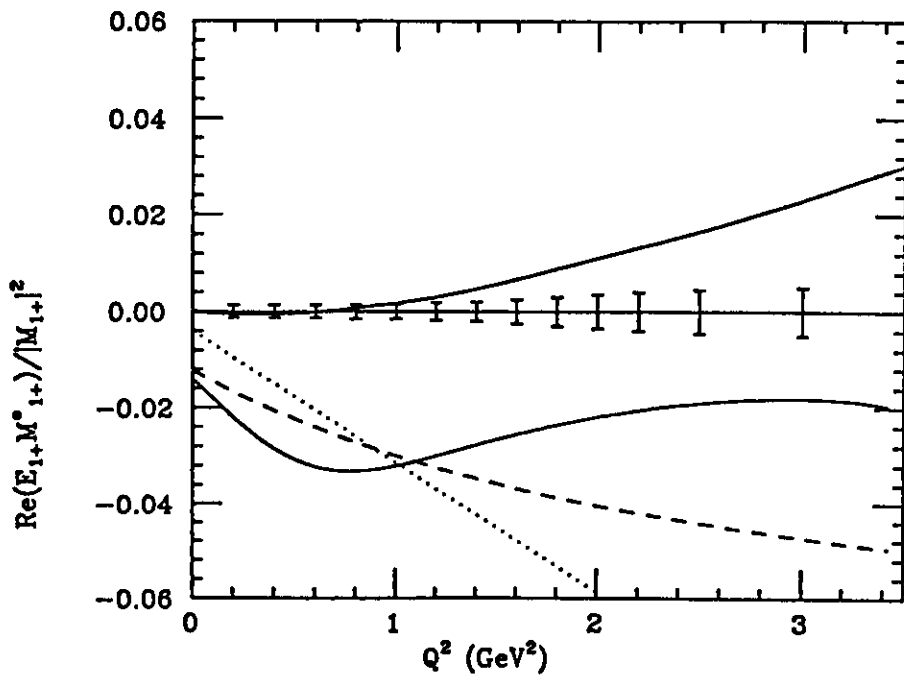
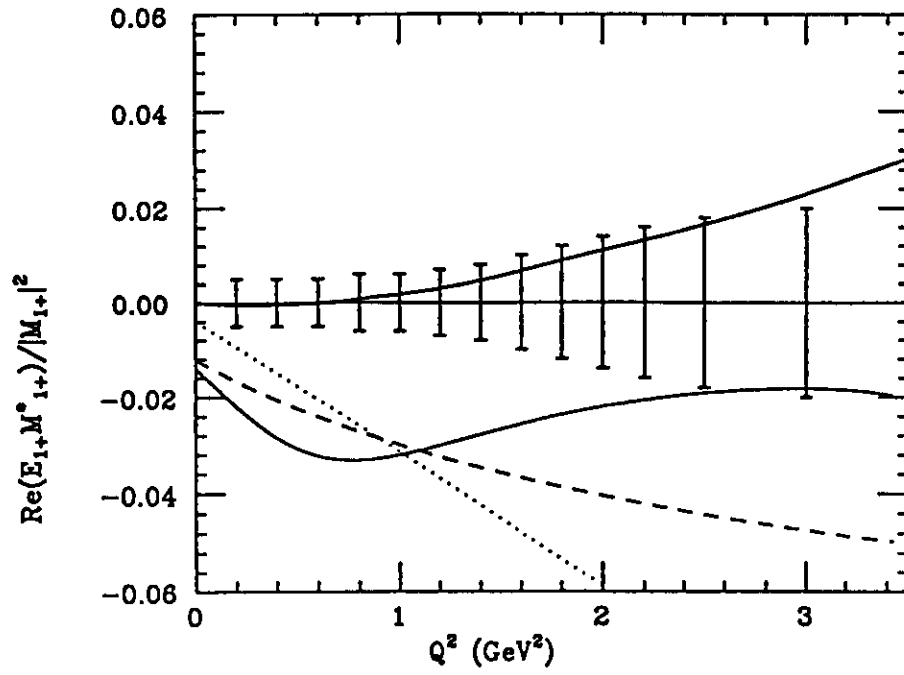


Figure 17. Expected statistical errors for the extraction of $\text{Re}(E_{1+} M_{1+}^*)$, for one acceptance bin (top) and for the complete fit.

Electroproduction: π^+ at $Q^2=1.0 \text{ GeV}^2/c^2$

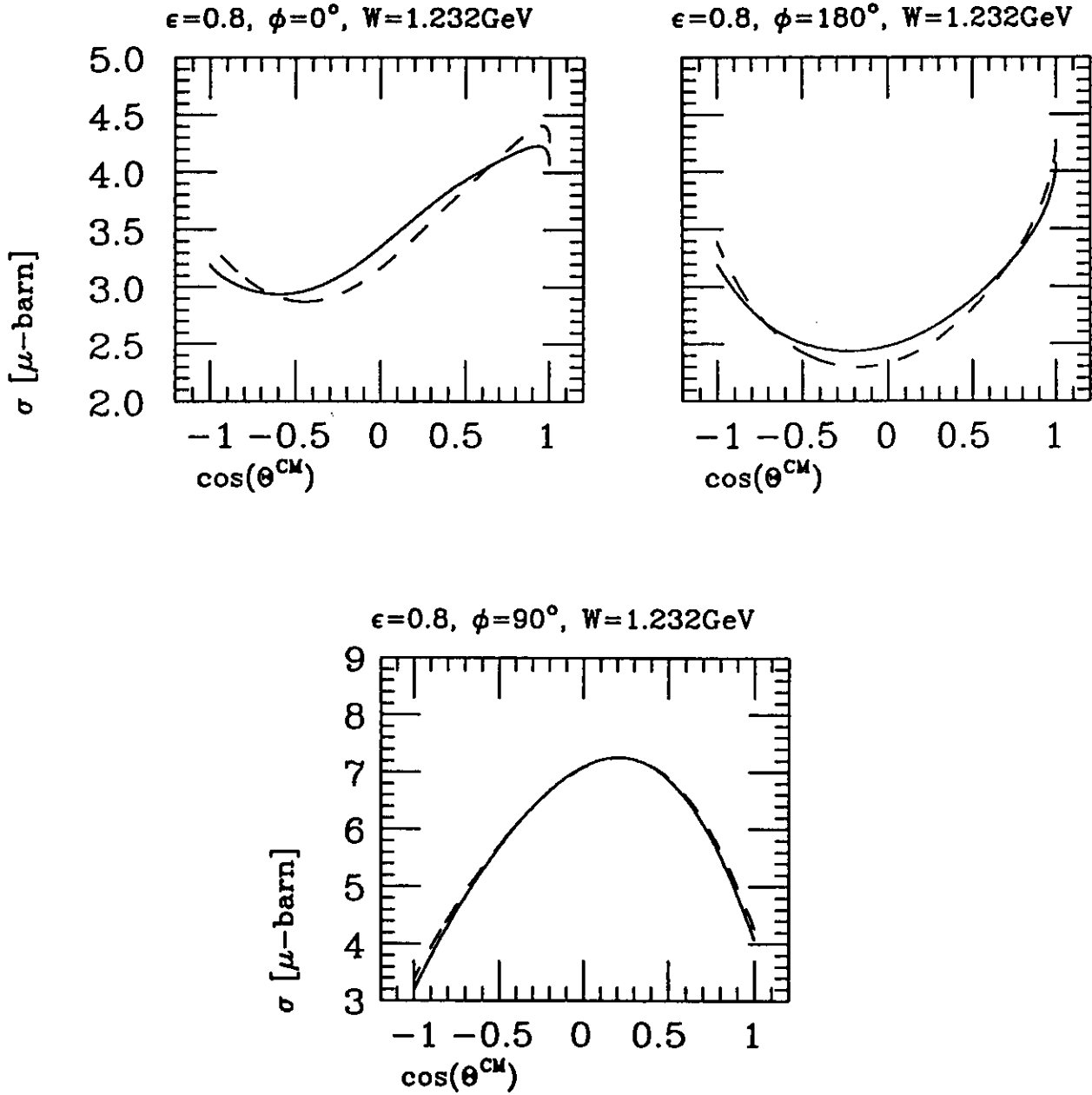


Figure 18. Same as in Figure 14, but for $p(e, e'\pi^+)n$.

Electroproduction: π^+ at $Q^2=1.0 \text{ GeV}^2/c^2$

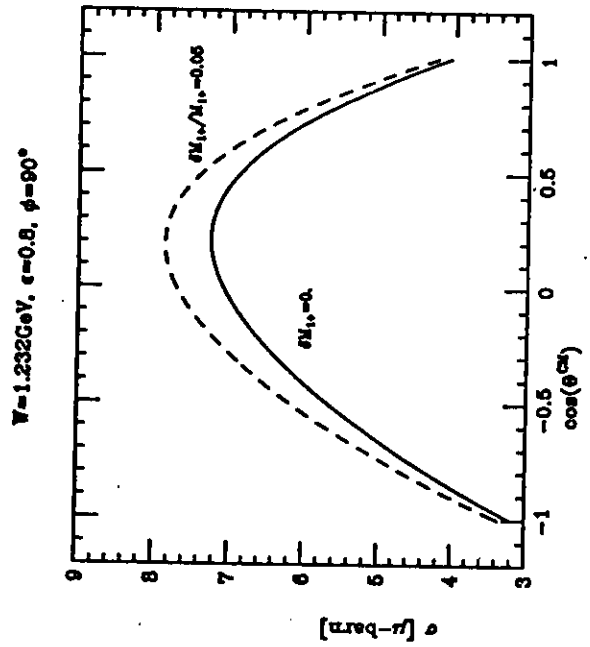
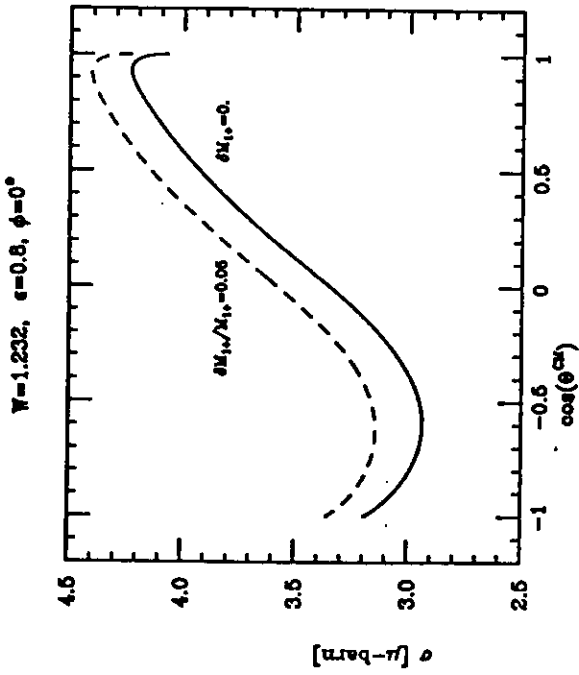
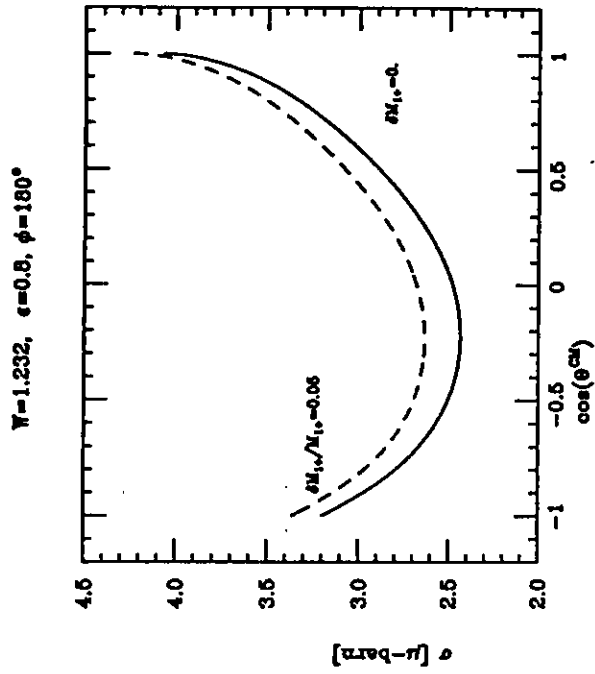


Figure 19. Same as in Figure 15, but for $p(e,e'\pi^+)n$.